

RESEARCH ARTICLE

Regulation of Hook1-mediated endosomal sorting of clathrin-independent cargo by γ -taxilin

Satoru Higashi, Tomohiko Makiyama*, Hiroshi Sakane[‡], Satoru Nogami[§] and Hiromichi Shirataki[¶]

ABSTRACT

In clathrin-independent endocytosis, Hook1, a microtubule- and cargo-tethering protein, participates in sorting of cargo proteins such as CD98 (encoded by *SLC3A2*) and CD147 (encoded by *BSG*) into recycling endosomes. However, the molecular mechanism that regulates Hook1-mediated endosomal sorting is not fully understood. In the present study, we found that γ -taxilin is a novel regulator of Hook1-mediated endosomal sorting. γ -Taxilin depletion promoted both CD98-positive tubular formation and CD98 recycling. Conversely, overexpression of γ -taxilin inhibited the CD98-positive tubular formation. Depletion of Hook1, or Rab10 or Rab22a (which are both involved in Hook1-mediated endosomal sorting), attenuated the effect of γ -taxilin depletion on the CD98-positive tubular formation. γ -Taxilin depletion promoted CD147-mediated spreading of HeLa cells, suggesting that γ -taxilin might be a pivotal player in various cellular functions in which Hook1-mediated cargo proteins are involved. γ -Taxilin bound to the C-terminal region of Hook1 and inhibited its interaction with CD98; the latter interaction is necessary for sorting CD98. We suggest that γ -taxilin negatively regulates the sorting of Hook1-mediated cargo proteins into recycling endosomes by interfering with the interactions between Hook1 and the cargo proteins.

KEY WORDS: Clathrin-independent endocytosis, Endosomal sorting, Hook1, Recycling endosome, Taxilin

INTRODUCTION

Endocytosis is involved in the maintenance of cellular homeostasis and the regulation of fundamental cellular functions including nutrient uptake, cell adhesion, cell migration, cell polarity, cytokinesis, and receptor signaling (Grant and Donaldson, 2009). Endocytosis is regulated by a series of trafficking processes including the internalization, sorting, degradation, and recycling of macromolecules. On the basis of the requirement for the coat protein clathrin for vesicle formation and internalization, endocytosis is classified into clathrin-mediated endocytosis (CME) and clathrin-independent endocytosis (CIE) (Grant and

Donaldson, 2009). CME has been studied extensively and is involved in the selective internalization of plasma membrane proteins such as transferrin and low-density lipoprotein receptor, both of which have distinct cytoplasmic sorting sequences that are recognized by adaptor proteins of the clathrin coat. After internalization, CME cargo proteins undergo a sorting process leading to transport to lysosomes for degradation, the *trans*-Golgi network, or recycling endosomes (REs) for return to the cell surface. By contrast, CIE had been studied as a non-selective bulk endocytic entry mechanism, and until 20 years ago, CIE cargo proteins did not appear to have a mechanism for selective internalization. However, increasing evidence has shown that CIE has a variety of entry mechanisms including caveolar endocytosis, RhoA-associated endocytosis, Cdc42-associated endocytosis, Arf6-associated endocytosis, and flotillin-associated endocytosis (Mayor et al., 2014). Moreover, it has been revealed in parallel with the growing number of known CIE cargo proteins that CIE cargo proteins are involved in a variety of vital physiological processes, including immune surveillance, cell migration, metastasis, and cell signaling. As the trafficking itineraries of endocytosed CIE cargo proteins (i.e. transport to lysosomes for degradation or REs for return to the cell surface) are thought to participate in regulation of the activities of the CIE cargo proteins, the molecular mechanisms of the endocytic trafficking processes of CIE after internalization have been studied extensively over the past decade.


The list of CIE cargo proteins identified so far is diverse, and includes major histocompatibility complex class I (MHC-I), glycosylphosphatidylinositol-anchored proteins (GPI-APs; CD55 and CD59), proteins involved in interactions with the extracellular matrix [CD44, CD98 (encoded by *SLC3A2*), CD147 (*BSG*), E-cadherin and β 1-integrin], ion channels [mucopolipin2 and Kir3.4 (encoded by *KCNJ5*)], and nutrient transporters [CD98 and Lat1 (encoded by *SLC7A5*)] (Grant and Donaldson, 2009; Mayor et al., 2014). It has been revealed that there are at least two endocytic trafficking pathways for CIE cargo proteins after internalization (Maldonado-Báez et al., 2013a,b). CIE cargo protein-loaded vesicles first mature into or fuse with Rab5-positive early endosomes (EEs). Then, a group of CIE cargo proteins (MHC-I and CD55) is transported to Rab5- and early endosome-associated antigen 1 (EEA1)-positive EEs, followed by co-localization with transferrin, a CME cargo protein. From there, the CIE cargo proteins are transported to late endosomes (LEs) and lysosomes for degradation, or to REs for recycling back to the plasma membrane. Another group of CIE cargo proteins (CD44, CD98, and CD147) is directly sorted into REs and recycled back to the plasma membrane in a Hook1- and Rab22a-dependent manner.

In mammals, the Hook family is comprised of Hook1, Hook2, and Hook3. Hook1 was initially identified in *Drosophila melanogaster* as a pivotal player in the delivery of internalized proteins to LEs (Krämer and Phistry, 1996; Sunio et al., 1999). Hook1 has a long coiled-coil region and interacts with microtubules

Department of Molecular and Cell Biology, Graduate School of Medicine, Dokkyo Medical University, 880 Kitakobayashi, Mibu-machi, Tochigi 321-0293, Japan.

*Present address: Division of Biological Chemistry, Department of Pharmaceutical Sciences, Showa University School of Pharmacy, 1-5-8 Hatanodai, Shinagawa-ku, Tokyo 142-8555, Japan. [‡]Present address: Faculty of Pharmacy and Pharmaceutical Sciences, Fukuyama University, Fukuyama, Hiroshima 729-0292, Japan. [§]Present address: Graduate School of Science, The University of Tokyo, Bunkyo-ku, Tokyo 113-0033, Japan.

[¶]Author for correspondence (hiro-sh@dokkyomed.ac.jp)

 S.H., 0000-0002-3353-1495; S.N., 0000-0002-4517-0180; H.Shirataki, 0000-0002-6291-6829

Handling Editor: Mahak Sharma

Received 29 April 2021; Accepted 30 November 2021

and organelle membranes through its N-terminal and C-terminal regions, respectively, to facilitate the attachment of organelles to microtubules (Krämer and Phistry, 1999). Loss of Hook1 function in mice results in ectopic positioning of microtubular structures within the spermatid and causes an abnormal spermatozoon head shape phenotype (Mendoza-Lujambio et al., 2002). Hook2 is localized at centrosomes through its interaction with CEP110 (encoded by *CNTRL*) and participates in ciliogenesis (Baron Gaillard et al., 2011; Szebenyi et al., 2007). Hook3 participates in localization of the Golgi complex through its interaction with microtubules (Walenta et al., 2001). It has been revealed that Hook1 plays a role as a microtubule- and cargo-tethering factor in the recycling of some CIE cargo proteins (CD44, CD98, and CD147), but not of MHC-I or CD55 (Maldonado-Báez et al., 2013a,b). Hook1 interacts with the cytoplasmic sequence of CD98 and CD147 through its C-terminal domain and facilitates their recycling in coordination with Rab22a and the microtubule network (Maldonado-Báez et al., 2013a).

The Rab family, a member of the Ras small G protein superfamily, includes at least 70 members in mammals and is implicated in intracellular vesicle trafficking, such as exocytosis, endocytosis, and transcytosis (Zhen and Stenmark, 2015). A group of Rab family members including Rab5, Rab8a, Rab10, Rab11, Rab21, Rab22a, and Rab35 is implicated in endocytic trafficking processes of CIE cargo proteins (Del Olmo et al., 2019; Dutta and Donaldson, 2015; Etoh and Fukuda, 2019; Grant and Donaldson, 2009; Rahajeng et al., 2012; Sharma et al., 2009; Solis et al., 2013; Weigert et al., 2004). Together with Hook1 and microtubules, Rab22a functions in recycling to the plasma membrane of CIE cargo proteins, including CD44, CD98, and CD147. It has been shown that although REs appear as both vesicular and tubular endosomes, the tubular formation of REs is crucial for the recycling back to the plasma membrane of CIE cargo proteins, and that Rab22a mediates the formation of tubular REs in coordination with Hook1 and the microtubule network (Maldonado-Báez et al., 2013a).

The taxilin family is composed of at least three members, α -taxilin, β -taxilin and γ -taxilin (also known as FIAT), which share a C-terminal long coiled-coil region (Nogami et al., 2004). In mammals, α - and γ -taxilin are ubiquitously expressed (Horii et al., 2014; Nogami et al., 2003), whereas β -taxilin is specifically expressed in skeletal muscle and heart (Sakane et al., 2016). Extensive studies by our group and others over the past decade have uncovered the function of the taxilin family members as follows. α -Taxilin was initially identified as a binding partner of the syntaxin family that participates in intracellular vesicle trafficking. It is also involved in the recycling pathway of the transferrin receptor (TfnR) through interaction with sorting nexin-4 (Sakane et al., 2014). Moreover, α -taxilin participates in intracellular trafficking of hepatitis B virus DNA-containing particles (Hoffmann et al., 2013). Interestingly, α -taxilin is specifically expressed in proliferating cells of the gastrointestinal tract (Horii et al., 2014) and overexpressed in various tumor types such as hepatocellular carcinoma, renal cell carcinoma, and glioblastoma (Mashidori et al., 2011; Oba-Shinjo et al., 2005; Ohtomo et al., 2010), suggesting that α -taxilin might be involved in cell proliferation. β -Taxilin participates in differentiation of C2C12 myoblasts into myotubes by suppressing the function of dysbindin (Sakane et al., 2016). γ -Taxilin is localized to the centrosome during interphase and participates in Nek2A-mediated centrosome disjunction as a negative regulator (Makiyama et al., 2018). Moreover, γ -taxilin is implicated in hypoxia-induced endoplasmic reticulum (ER) stress responses (Hotokezaka et al., 2015) and interacts with activating

transcription factor 4 (ATF4) to repress its transcriptional activity in osteoblasts (Yu et al., 2005, 2008).

The function of α -taxilin in intracellular vesicle trafficking prompted us to examine whether γ -taxilin is also involved in processes of intracellular vesicle trafficking. In the present study, we identify Hook1 as a novel binding partner of γ -taxilin. Depletion of γ -taxilin prompted tubular formation of REs harboring CD98 or CD147, Hook1-mediated cargo proteins, leading to enhancement of the recycling of these cargo proteins back to the plasma membrane. Moreover, depletion of γ -taxilin prompted CD147-mediated spreading of HeLa cells, probably by enhancing Hook1-mediated recycling of CD147 back to the plasma membrane. Conversely, overexpression of γ -taxilin inhibited the tubular formation of CD98-positive REs through interaction with the C-terminal region of Hook1 competitively with CD98. We propose that γ -taxilin negatively regulates the sorting of Hook1-mediated CIE cargo proteins into REs by interfering with the interactions between Hook1 and CIE cargo proteins.

RESULTS

γ -Taxilin interacts with Hook1 and Hook2

As α -taxilin interacts with sorting nexin-4 and participates in the recycling pathway of TfnR (Sakane et al., 2014), we postulated that γ -taxilin might also be involved in intracellular vesicle traffic. To test this possibility, we first attempted to identify γ -taxilin-interacting molecules by use of yeast two-hybrid screening using full-length γ -taxilin as bait and found that Hook1, a microtubule- and cargo-tethering protein, was a potential binding partner of γ -taxilin. Hook1 interacted with γ -taxilin but not α - or β -taxilin (Fig. 1A). When we examined the interactions between taxilin family members and other Hook family proteins, only γ -taxilin interacted with Hook2, and none of the taxilins interacted with Hook3 (Fig. 1A). Consistently, when human influenza hemagglutinin (HA)-tagged α -, β -, or γ -taxilin and myc-tagged Hook1, Hook2, or Hook3 were co-expressed in HeLa cells and the cell lysates were immunoprecipitated with anti-HA or anti-myc antibodies, myc-Hook1 and -Hook2 were co-immunoprecipitated with HA- γ -taxilin and vice versa (Fig. 1B). Although it is possible that the interaction of γ -taxilin with Hook2 may provide a clue to the role of γ -taxilin in centrosomes, we focused here on the interaction of γ -taxilin with Hook1 and proceeded with examinations to reveal whether γ -taxilin is implicated in Hook1-related intracellular vesicle trafficking. We first attempted to detect the interaction between endogenous γ -taxilin and Hook1 using an immunoprecipitation assay and found that endogenous Hook1 was co-immunoprecipitated with endogenous γ -taxilin (Fig. 1C). Immunocytochemical analysis revealed that endogenous γ -taxilin and Hook1 showed a similar staining pattern (Fig. 1D). Since both of the available anti- γ -taxilin and anti-Hook1 antibodies were unfortunately produced in rabbit, we examined whether GFP- γ -taxilin and myc-Hook1 are co-localized in HeLa cells. Immunocytochemical analysis showed that the staining patterns of GFP- γ -taxilin and myc-Hook1 were similar to those of the corresponding endogenous proteins and GFP- γ -taxilin was co-localized with myc-Hook1 (Fig. 1E).

γ -Taxilin depletion promotes the tubular formation of Hook1-mediated cargo proteins

Hook1 was originally discovered in *Drosophila melanogaster* as a microtubule- and cargo-tethering protein for the delivery of plasma membrane receptors to late endosomal compartments, and increasing evidence highlights a role of Hook1 in the sorting of a

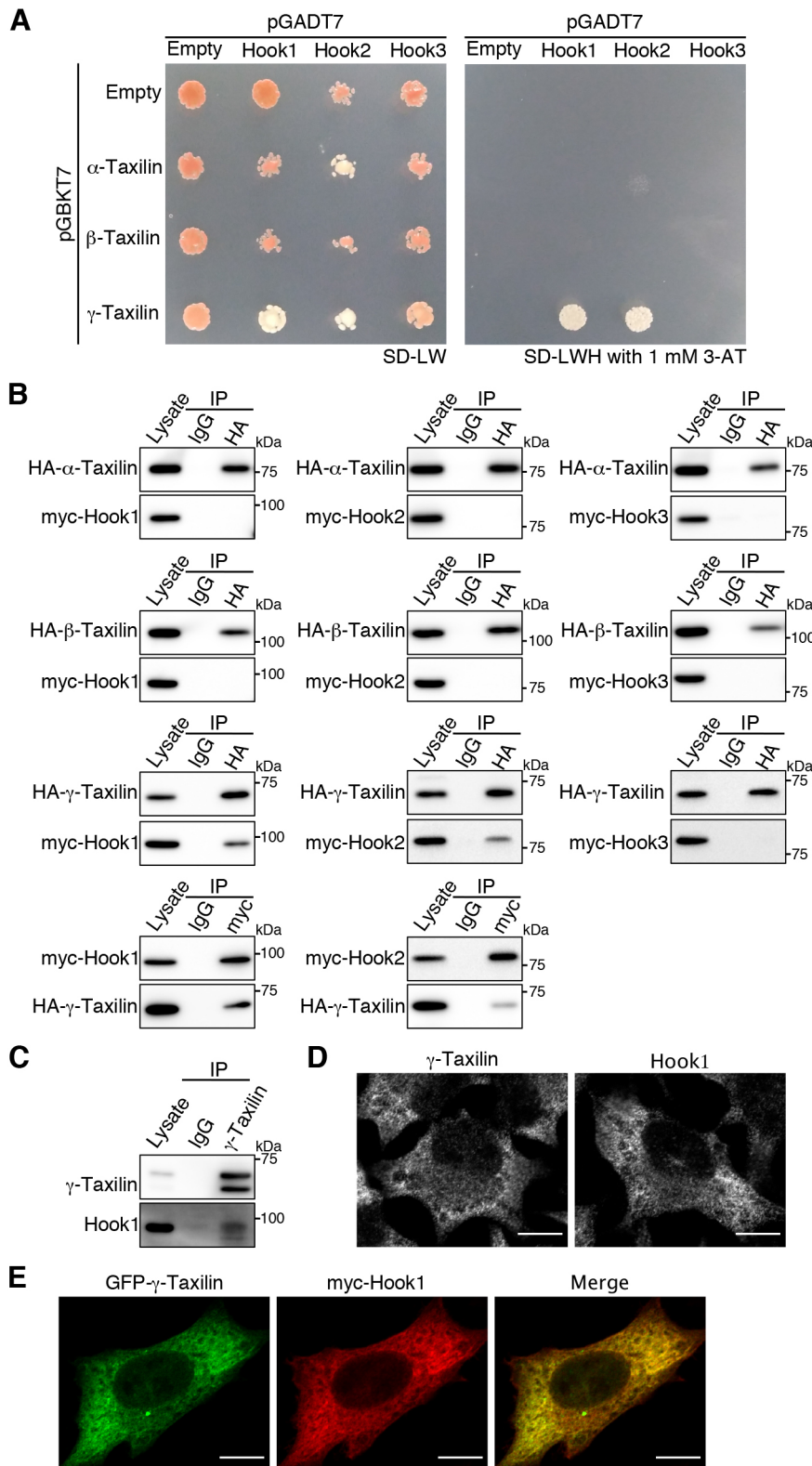


Fig. 1. γ -Taxilin interacts with Hook1 and Hook2 but not Hook3. (A) Yeast two-hybrid assay. pGBKT7 harboring a cDNA fragment encoding α -, β -, or γ -taxilin, and pGADT7 harboring a cDNA fragment encoding Hook1, Hook2, or Hook3 were co-introduced into yeast reporter strain Y2H Gold. Equal amounts of the indicated transformants were spotted on to synthetic defined medium (SD) –LW (non-selective) or SD –LWH with 3-amino-1, 2, 4-triazole (3-AT) (selective) plates. Images are representative of three independent experiments. (B,C) Co-immunoprecipitation assay. Cell lysates of HeLa cells co-transfected with HA-tagged α -, β -, or γ -taxilin and myc-tagged Hook1, Hook2, or Hook3 (B) or not (C) were immunoprecipitated using the indicated antibodies. The immunoprecipitate was subjected to SDS-PAGE followed by western blotting with indicated antibodies for detection of corresponding proteins ($n=3$, each experiment). The amount of cell lysates used for western blotting were 2.5% (B) or 1.25% (C) of those used for immunoprecipitation (IP). (D,E) Immunocytochemistry. HeLa cells were immunostained with an anti- γ -taxilin or anti-Hook1 antibody in D. HeLa cells expressing GFP- γ -taxilin (green) and myc-Hook1 were immunostained with an anti-Hook1 antibody (red) in E. Images are representative of three independent experiments. Scale bars: 10 μ m.

subset of CIE cargo proteins (e.g. CD98, CD147) into REs in mammals (Maldonado-Báez et al., 2013a). Using small interfering RNA (siRNA), we examined whether γ -taxilin is involved in the Hook1-mediated sorting of CIE cargo proteins into REs. The efficiency of γ -taxilin depletion was first assessed by immunoblotting. In γ -taxilin siRNA-treated cells, γ -taxilin was

depleted below the detection level (Fig. 2A), whereas other proteins including Hook1, CD98, CD147, and glyceraldehyde 3-phosphate dehydrogenase (GAPDH) were not affected (Fig. S1). To label the Hook1-mediated CIE system, siRNA-treated cells were incubated with an anti-CD98 antibody at 37°C for 1 h to allow internalization of the antibody-bound CD98, and internalized CD98 was

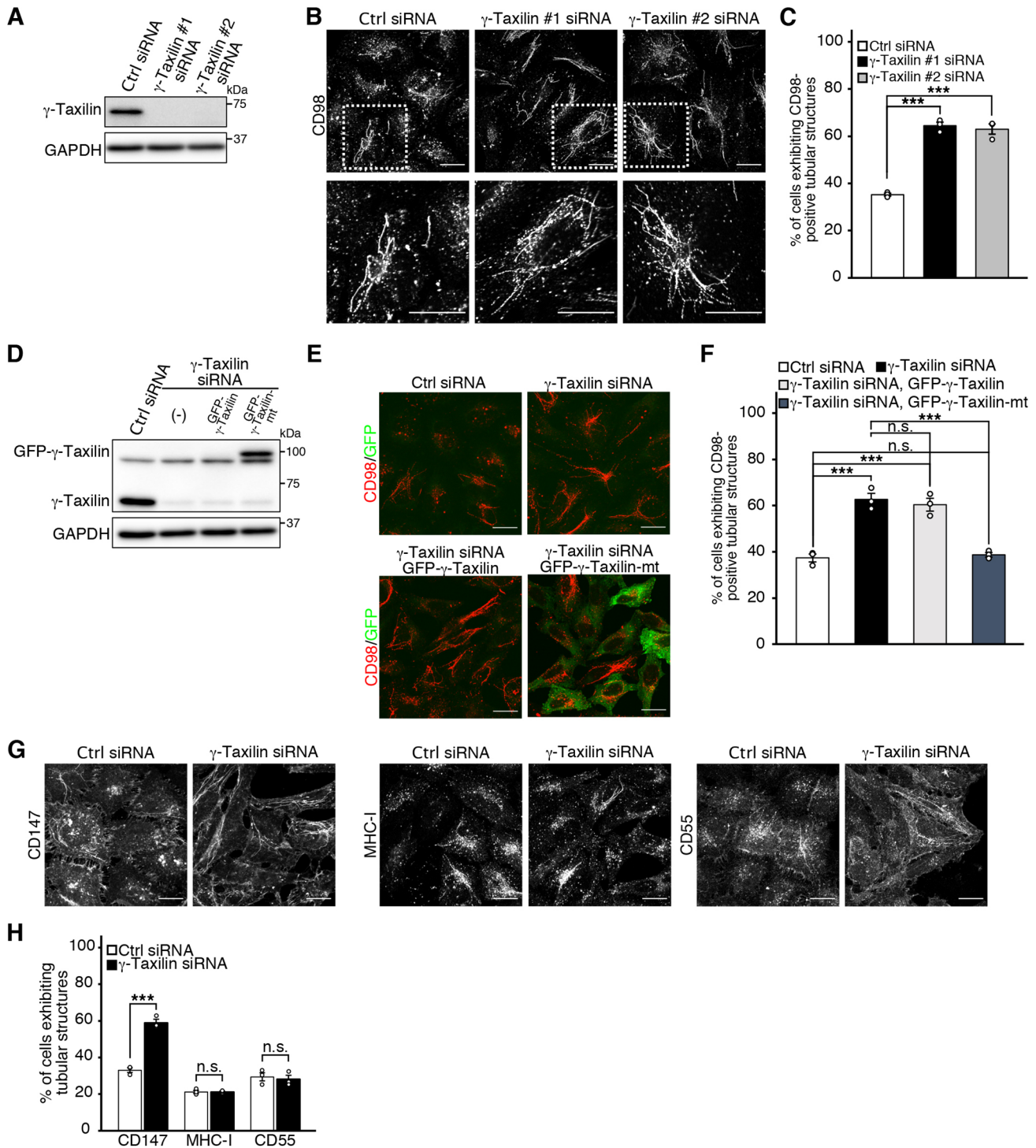


Fig. 2. γ -Taxilin depletion promotes the tubular formation of Hook1-mediated cargo proteins. (A) Depletion of γ -taxilin by siRNA. HeLa cells were transfected with control (Ctrl) or γ -taxilin (γ -Taxilin #1 or #2) siRNA. Cell lysates were subjected to SDS-PAGE followed by western blotting with the indicated antibodies. (B) Formation of CD98-positive tubular structures in the indicated siRNA-treated cells. Magnified views of the boxed areas in the upper panels are shown in the lower panels. Scale bars: 20 μ m. (C) Quantitative analysis of the formation of CD98-positive tubular structures in B. The percentages of cells exhibiting CD98-positive tubular structures are shown as the mean \pm s.e.m. ($n=3$; >100 cells were analyzed in each experiment). *** P <0.001 (two-tailed unpaired Student's t -test). (D) siRNA rescue experiments. γ -Taxilin siRNA-treated cells were transfected with the indicated plasmids at 24 h after treatment with γ -taxilin siRNA. Cell lysates were subjected to SDS-PAGE followed by western blotting with the indicated antibodies. (E) Formation of CD98-positive tubular structures in cells treated with the indicated siRNA and plasmids. Scale bars: 20 μ m. (F) Quantitative analysis of the formation of CD98-positive tubular structures in E. The percentages of cells exhibiting CD98-positive tubular structures are shown as the mean \pm s.e.m. ($n=3$; >100 cells were analyzed in each experiment). *** P <0.001; n.s., not significant (one-way ANOVA with post-hoc Tukey's multiple comparison test). (G) Formation of CD147-, MHC-I-, or CD55-positive tubular structures in the indicated siRNA-treated cells. Scale bars: 20 μ m. (H) Quantitative analyses of the formation of CD147-, MHC-I-, or CD55-positive tubular structures in D. The percentages of cells exhibiting CD147-, MHC-I-, or CD55-positive tubular structures are shown as the mean \pm s.e.m. ($n=3$; >100 cells were analyzed in each experiment). *** P <0.001; n.s., not significant (two-tailed unpaired Student's t -test).

specifically detected by immunostaining as described in the Materials and Methods section (Fig. 2B). Internalized CD98 was found in discrete punctate structures in control cells but also in tubular structures in about 35% of these cells (Fig. 2C). There was no difference in the expression levels of γ -taxilin between cells with or without CD98-positive tubular structures (data not shown). γ -Taxilin depletion caused an \sim 1.8-fold increase in the percentage of cells exhibiting CD98-positive tubular structures (Fig. 2C). As described previously, these tubular structures are not an artifact of immunostaining (Weigert et al., 2004), and they were also visualized by time-lapse imaging of living cells (see below). A similar result was obtained using another γ -taxilin siRNA. Moreover, when siRNA rescue experiments were performed using cells expressing siRNA-resistant γ -taxilin, the effect of γ -taxilin siRNA treatment on the formation of CD98-positive tubular structures was attenuated in siRNA-resistant γ -taxilin expression plasmid (pEGFPC1- γ -taxilin-*mt*)-transfected cells but not pEGFPC1- γ -taxilin-transfected cells (Fig. 2E,F). GFP- γ -taxilin was expressed in pEGFPC1- γ -taxilin-*mt*-transfected cells but not pEGFPC1- γ -taxilin-transfected cells (Fig. 2D). Taken together, the effect of γ -taxilin depletion on the formation of CD98-positive tubular structures is not caused by an off-target effect of siRNA treatment. These results suggest that γ -taxilin is involved in the Hook1-mediated sorting of CIE cargo protein CD98 into REs. We thus examined by use of siRNA whether γ -taxilin also affects the Hook1-mediated sorting of another CIE cargo protein into REs. When a similar experiment to that described above was performed using anti-CD147 antibody instead of anti-CD98 antibody, γ -taxilin depletion caused an \sim 1.8-fold increase in the percentage of cells exhibiting CD147-positive tubular structures (Fig. 2G,H).

It has been revealed that besides the CIE cargo proteins that are sorted into REs mediated by Hook1, another subset of CIE cargo proteins (e.g. MHC-I, CD55) are sorted into REs independently of Hook1 (Maldonado-Báez et al., 2013a). We performed similar experiments to those described above to determine whether γ -taxilin is involved in the sorting of MHC-I and CD55 into REs. γ -Taxilin depletion did not affect the percentage of cells exhibiting MHC-I- or CD55-positive tubular structures (Fig. 2G,H). Taken together, we suggest that γ -taxilin specifically participates in the Hook1-mediated tubular formation of CIE cargo proteins.

The effect of γ -taxilin depletion on Hook1-mediated tubular formation is attenuated by co-depletion of Hook1, Rab10 or Rab22a

To validate the involvement of γ -taxilin in Hook1-mediated sorting of CIE cargo proteins into REs, we examined whether Hook1 depletion affects the effect of γ -taxilin depletion on the formation of CD98-positive tubular structures. In Hook1 siRNA-treated cells, Hook1 was depleted below the detection level, whereas γ -taxilin and GAPDH were not affected (Fig. 3A). γ -Taxilin depletion did not affect the expression level of Hook1 (Fig. 3A). Hook1 depletion alone significantly decreased the percentage of cells exhibiting CD98-positive tubular structures (Fig. 3B,C). Simultaneous depletion of Hook1 and γ -taxilin significantly decreased the percentage of cells exhibiting CD98-positive tubular structures, to a similar level to that observed on Hook1 depletion alone, whereas γ -taxilin depletion increased the percentage of those cells (Fig. 3B,C).

It has been revealed that Rab22a participates in Hook1-mediated sorting of CIE cargo proteins into REs, and shown that Rab22a depletion decreases the percentage of cells exhibiting CD98-positive tubular structures (Maldonado-Báez et al., 2013a). To further test the possibility that γ -taxilin participates in Hook1-

mediated sorting of CIE cargo proteins into REs, we examined whether Rab22a depletion influences the effect of γ -taxilin depletion on the formation of CD98-positive tubular structures. In Rab22a siRNA-treated cells, Rab22a was depleted below the detection level, whereas γ -taxilin and GAPDH were not affected (Fig. 3A). γ -Taxilin depletion did not affect the expression level of Rab22a (Fig. 3A). Rab22a depletion alone significantly decreased the percentage of cells exhibiting CD98-positive tubular structures (Fig. 3B,C). Simultaneous depletion of Rab22a and γ -taxilin significantly decreased the percentage of cells exhibiting CD98-positive tubular structures, to a similar level to that observed on Rab22a depletion alone (Fig. 3B,C).

Moreover, it has recently been shown that Rab10 is involved in the tubular formation of MICAL-L1-positive REs (MICAL-L1 is an RE marker), and that overexpressed Rab10 co-localizes with CD147 at tubular REs (Etoh and Fukuda, 2019). We speculated that Rab10 is also involved in Hook1-mediated sorting of CIE cargo proteins into REs and performed similar experiments to those described above but using Rab10 siRNA instead of Rab22a siRNA. In Rab10 siRNA-treated cells, Rab10 was depleted below the detection level, whereas γ -taxilin and GAPDH were not affected (Fig. 3A). γ -Taxilin depletion did not affect expression level of Rab10 (Fig. 3A). Rab10 depletion alone significantly decreased the percentage of cells exhibiting CD98-positive tubular structures (Fig. 3B,C). Simultaneous depletion of Rab10 and γ -taxilin significantly decreased the percentage of cells exhibiting CD98-positive tubular structures, to a similar level observed on Rab10 depletion alone (Fig. 3B,C). Taken together, we suggest that γ -taxilin functionally interacts with Hook1 in the Hook1-mediated tubular formation of CIE cargo proteins.

γ -Taxilin depletion promotes the biogenesis of CD98-positive tubules

On the basis of the results above, γ -taxilin might regulate the biogenesis of CD98-positive tubules. To test this possibility, we first prepared an Alexa Fluor 488-labeled anti-CD98 antibody, and cells treated with control or γ -taxilin siRNA were incubated with the labeled anti-CD98 antibody at 37°C for 1 h to allow internalization of antibody-bound CD98. After washing out antibody remaining on the cell surface, the labeled antibody-bound CD98 was observed. At the start of observation (time zero), internalized CD98 prominently appeared in discrete punctate structures, but CD98-positive tubules were also observed in each treated cell. These observations are consistent with the immunostaining pattern of internalized CD98 shown in Fig. 2B. To analyze the formation of CD98-positive tubules, time-lapse images were captured at 10-s intervals over 10 min (Fig. 4A; Movies 1 and 2). We measured the length of newly formed CD98-positive tubules during the period of observation; these tubules were categorized into five groups by their maximum length (<5 μ m, 5–10 μ m, 11–15 μ m, 16–20 μ m, and >20 μ m). In our experimental conditions, γ -taxilin depletion resulted in an \sim 1.9-fold increase in the average number of newly formed CD98-positive tubules per cell (Fig. 4B), and the number of newly formed CD98-positive tubules >20 μ m long significantly increased in γ -taxilin-depleted cells compared with control cells (Fig. 4C). In addition, we examined whether γ -taxilin depletion affects the frequency of CD98-positive tubule collapse. There was no significant difference in the frequency of CD98-positive tubule collapse between control and γ -taxilin-depleted cells (data not shown). These results indicate that γ -taxilin regulates the number and length of CD98-positive tubules, suggesting that γ -taxilin may inhibit the biogenesis of Hook1-mediated cargo protein-positive tubules.

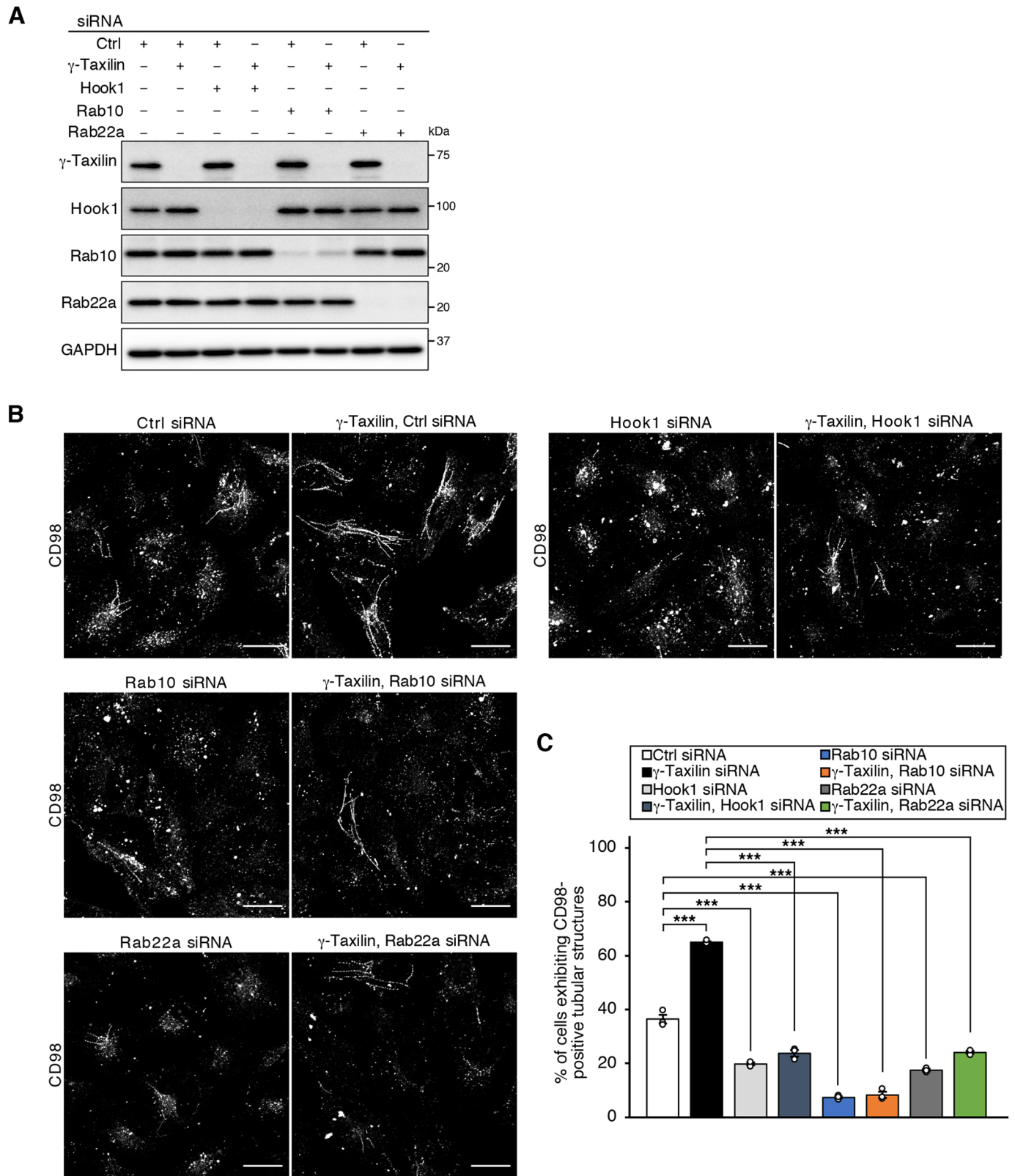


Fig. 3. The effect of γ -taxilin depletion on the formation of CD98-positive tubular structures is attenuated by co-depletion of Hook1, Rab10, or Rab22a. (A) Co-depletion of γ -taxilin and Hook1, Rab10, or Rab22a by siRNA. HeLa cells were transfected with control (Ctrl) or γ -taxilin (γ -taxilin #1) siRNA and Hook1, Rab10, or Rab22a siRNA. Cell lysates were subjected to SDS-PAGE followed by western blotting with the indicated antibodies. Blots are representative of three independent experiments. (B) Formation of CD98-positive tubular structures in the indicated siRNA-treated cells. Scale bars: 20 μ m. (C) Quantitative analysis of the formation of CD98-positive tubular structures in B. The percentages of cells exhibiting CD98-positive tubular structures are shown as the mean \pm s.e.m. ($n=3$; >100 cells were analyzed in each experiment). *** $P<0.001$ (one-way ANOVA with post-hoc Tukey's multiple comparison test).

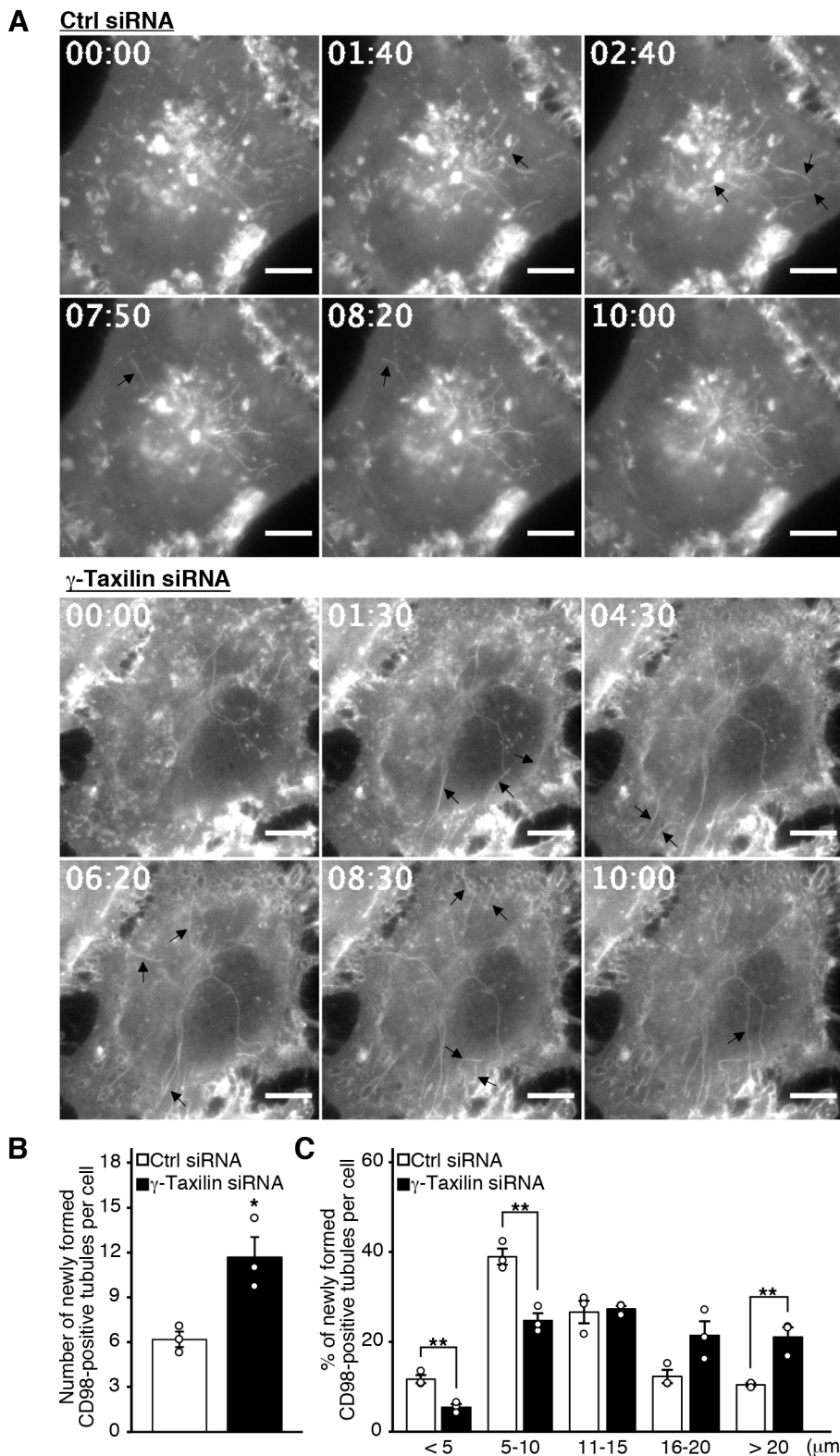


Fig. 4. γ -Taxilin depletion promotes the biogenesis of CD98-positive tubules.

(A) Dynamics of CD98-positive tubules in the indicated siRNA-treated cells. Time-lapse images were captured at 10-s intervals over 10 min. Arrows indicate newly formed CD98-positive tubules. Scale bars: 10 μ m. (B) Quantitative analysis of the number of newly formed CD98-positive tubules in A. The number of CD98-positive tubules newly formed during the period of observation is shown as the mean \pm s.e.m. ($n=3$; >10 cells were analyzed in each experiment). * $P<0.05$ (two-tailed unpaired Student's t -test). (C) Histogram analysis of the length of newly formed CD98-positive tubules in A. The length of each CD98-positive tubule newly formed during the period of observation was measured. Newly formed CD98-positive tubules were categorized into groups by maximum length (<5 μ m, 5–10 μ m, 11–15 μ m, 16–20 μ m, and >20 μ m). The percentages of the categorized tubules per cell are shown as the mean \pm s.e.m. ($n=3$; >10 cells were analyzed in each experiment). ** $P<0.01$ (two-tailed unpaired Student's t -test).

γ -Taxilin depletion promotes the recycling of CD98 to the plasma membrane

Our results so far cannot eliminate the possibility that γ -taxilin might be indirectly involved in the Hook1-mediated biogenesis of tubular structures by affecting the internalization of CIE cargo proteins. Thus, we next examined by use of siRNA whether γ -taxilin affects the internalization of CD98. To label CD98 on the cell

surface, cells treated with control or γ -taxilin siRNA were incubated with anti-CD98 antibody for 1 h at 4°C. After washing out unbound antibody, the cells were further incubated for various time periods at 37°C to allow internalization of the antibody-bound CD98. To measure the intensity of antibody-bound CD98 on the cell surface before its internalization (time zero), cells were fixed and stained without permeabilization. There was no difference in the intensity of

antibody-bound CD98 on the cell surface between control and γ -taxilin siRNA-treated cells (Fig. S2A,B). Next, to measure the intensity of internalized antibody-bound CD98, cells were fixed and stained with permeabilization. The intensity of internalized antibody-bound CD98 increased in a time-dependent manner and was not altered in γ -taxilin-depleted cells compared with control cells (Fig. S2A,C). This result indicates that γ -taxilin is not involved in the internalization of CD98, suggesting that γ -taxilin directly affects the Hook1-mediated biogenesis of tubular structures.

Taken together with the report that increased Hook1-mediated biogenesis of tubular structures results in increased recycling of Hook1-mediated cargo proteins to the plasma membrane (Maldonado-Báez et al., 2013a), our results raise the possibility that γ -taxilin may affect the recycling of Hook1-mediated cargo proteins to the plasma membrane. Thus, we examined by use of siRNA whether γ -taxilin affects the recycling of CD98 to the plasma membrane. Cells treated with control or γ -taxilin siRNA were incubated with anti-CD98 antibody for 1 h at 37°C to allow internalization of the antibody-bound CD98. After washing out antibody remaining on the cell surface, the cells were further incubated for various time periods at 37°C to allow recycling of the internalized antibody-bound CD98 to the plasma membrane. As antibody-bound CD98 recycled back to the plasma membrane remains on the cell surface, the cells were fixed and stained without permeabilization to detect it. To detect antibody-bound CD98 in intracellular compartments, cells were fixed and stained with permeabilization after washing out antibody recycled back to the cell surface. The intensity of internalized antibody-bound CD98 before its recycling to the plasma membrane (time zero) was not altered in γ -taxilin siRNA-treated cells compared with control cells (Fig. S3A). Then, the intensity of internalized antibody-bound CD98 at time zero was set to 1.0 for control and γ -taxilin-depleted cells respectively, and the intensities of antibody-bound CD98 were determined at various time periods relative to that of internalized antibody-bound CD98 at time zero. The intensities of antibody-bound CD98 remaining in the intracellular compartments and antibody-bound CD98 recycled back to the plasma membrane are shown in Fig. 5E,F, respectively. In γ -taxilin-depleted cells, the intensity of antibody-bound CD98 remaining in the intracellular compartments significantly decreased in a time-dependent manner compared with control cells (Fig. 5A,E). Conversely, in γ -taxilin-depleted cells, the intensity of antibody-bound CD98 recycled back to the plasma membrane significantly increased in a time-dependent manner compared with control cells (Fig. 5B,F). Taken together with the evidence that the increase in the intensity of antibody-bound CD98 recycled back to the plasma membrane was proportional to the decrease in the intensity of antibody-bound CD98 remaining in the intracellular compartments, these results indicate that γ -taxilin depletion promotes the recycling of CD98 to the plasma membrane.

We also examined whether γ -taxilin affects the recycling of MHC-I, which is sorted into REs independently of Hook1, to the plasma membrane. γ -Taxilin depletion did not affect the recycling of MHC-I to the plasma membrane (Fig. 5C,D,G,H; Fig. S3B), suggesting that γ -taxilin specifically participates in the recycling of Hook1-mediated cargo proteins to the plasma membrane.

Finally, to determine whether γ -taxilin participates in the recycling of CME cargo proteins to the plasma membrane, we examined the effect of γ -taxilin depletion on the recycling of endocytosed TfnR to the plasma membrane. After serum starvation for 30 min at 37°C, cells treated with control or γ -taxilin siRNA were incubated with Alexa Fluor 594-labeled transferrin (Tfn-594)

for 1 h at 37°C. After washing out cell surface Tfn-594, the cells were further incubated for various time periods at 37°C to monitor recycling of Tfn-594 to the plasma membrane (Fig. S4A). The intensity of Tfn-594 at time zero was not affected by γ -taxilin depletion (Fig. S4B). The intensity of Tfn-594 at time zero was set to 1.0 for control and γ -taxilin-depleted cells, respectively, and the intensity of Tfn-594 at various time periods relative to that at time zero is shown in Fig. S4C. γ -Taxilin depletion did not affect the recycling of Tfn-594 to the plasma membrane (Fig. S4C), suggesting that γ -taxilin is not involved in the recycling of CME cargo proteins to the plasma membrane.

γ -Taxilin depletion promotes HeLa cell spreading mediated by CD147

The recycling of CD98 and CD147 to the plasma membrane participates in the activation of β 1-integrin and focal adhesion kinase (FAK) signaling mediated by cell spreading in human hepatocellular carcinoma SMMC-7721 cells (Wu et al., 2015, 2016). We examined by use of siRNA whether γ -taxilin is involved in the activation of β 1-integrin and FAK signaling mediated by spreading of HeLa cells. The phosphorylation of FAK on Tyr397, which is known as an initial step in the activation of β 1-integrin and FAK signaling mediated by cell spreading (Huveneers and Danen, 2009), was assessed by immunoblotting. γ -Taxilin depletion did not affect the basal FAK phosphorylation level in HeLa cells (Fig. S5A,B). However, when cells were detached from culture dishes followed by replating on glass coverslips to allow spreading on them, FAK phosphorylation levels were significantly increased in a time-dependent manner in γ -taxilin-depleted cells compared with control cells (Fig. 6A,B). Taken together with the result that γ -taxilin depletion promotes the recycling of CD98 to the plasma membrane, these results suggest that γ -taxilin depletion may enhance the activation of β 1-integrin and FAK signaling mediated by cell spreading through recycling of CD98 to the plasma membrane.

It has been revealed that the recycling of CIE cargo proteins to the plasma membrane is required for spreading of HeLa cells and that Hook1 depletion inhibits cell spreading (Maldonado-Báez et al., 2013a). As γ -taxilin depletion enhanced the activation of β 1-integrin and FAK signaling mediated by cell spreading, it is possible that γ -taxilin participates in cell spreading through the recycling of CIE cargo proteins to the plasma membrane. We thus examined by use of siRNA whether γ -taxilin is involved in spreading of HeLa cells (Fig. 6C,D). To assess cell spreading, cell area was measured. The average cell area was significantly increased in a time-dependent manner in γ -taxilin-depleted cells compared with control cells (Fig. 6E). Consistently, the average cell area at each time point was significantly lower for Hook1-depleted cells than control cells (Fig. 6E). The effect of γ -taxilin depletion on cell spreading was attenuated by simultaneous depletion of Hook1 (Fig. 6E). These results suggest that γ -taxilin is involved in spreading of HeLa cells by affecting the recycling of CIE cargo proteins that are sorted by Hook1.

We examined by use of siRNA which CIE cargo proteins are involved in spreading of HeLa cells. CD147 depletion significantly inhibited cell spreading, whereas CD98 depletion hardly affected cell spreading (Fig. 6E; Fig. S6). Next, we examined by use of siRNA whether CD147 is involved in the γ -taxilin-mediated cell spreading. The effect of γ -taxilin depletion on cell spreading was attenuated by simultaneous depletion of CD147 (Fig. 6E). In the above experiments, the treatment of cells with siRNA(s) induced depletion of the corresponding (target) proteins to below the

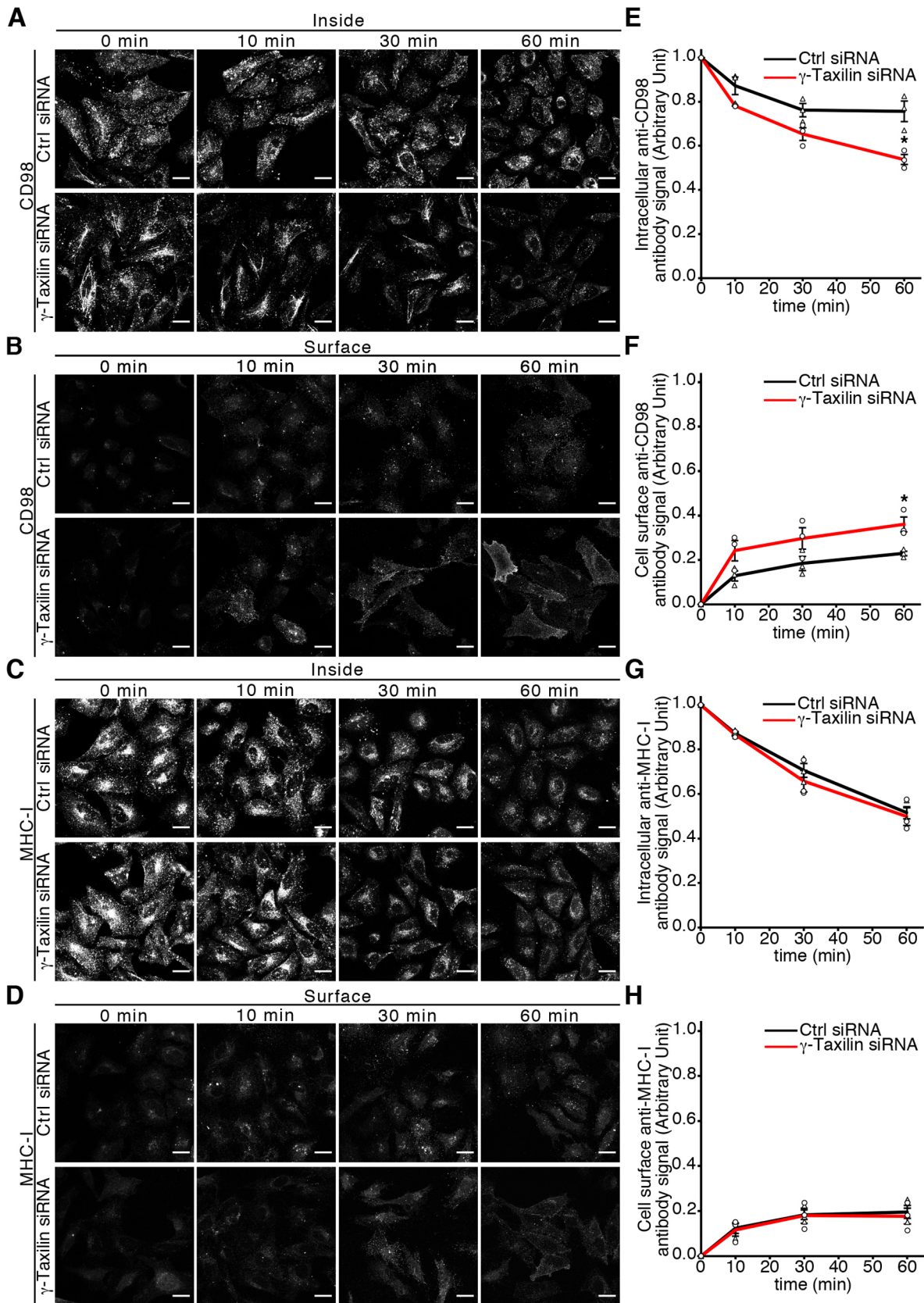


Fig. 5. γ -Taxilin depletion promotes recycling of CD98 but not MHC-I. (A–D) Recycling of CD98 (A,B) and MHC-I (C,D) in the indicated siRNA-treated cells. Scale bars: 20 μ m. (E–H) Quantitative analyses of recycling of CD98 (E,F) and MHC-I (G,H) in A and B, and C and D, respectively. Each antibody signal was measured as signal intensity per μ m². In E and G, results shown are the mean \pm s.e.m. of the ratio of the intracellular antibody signal at each time point to that at time zero. In F and H, results shown are the mean \pm s.e.m. of the ratio of the cell surface antibody signal at each time point to the intracellular antibody signal at time zero measured in experiments described in E and G ($n=3$; >40 cells were analyzed in each experiment). * $P<0.05$ (two-tailed unpaired Student's *t*-test).

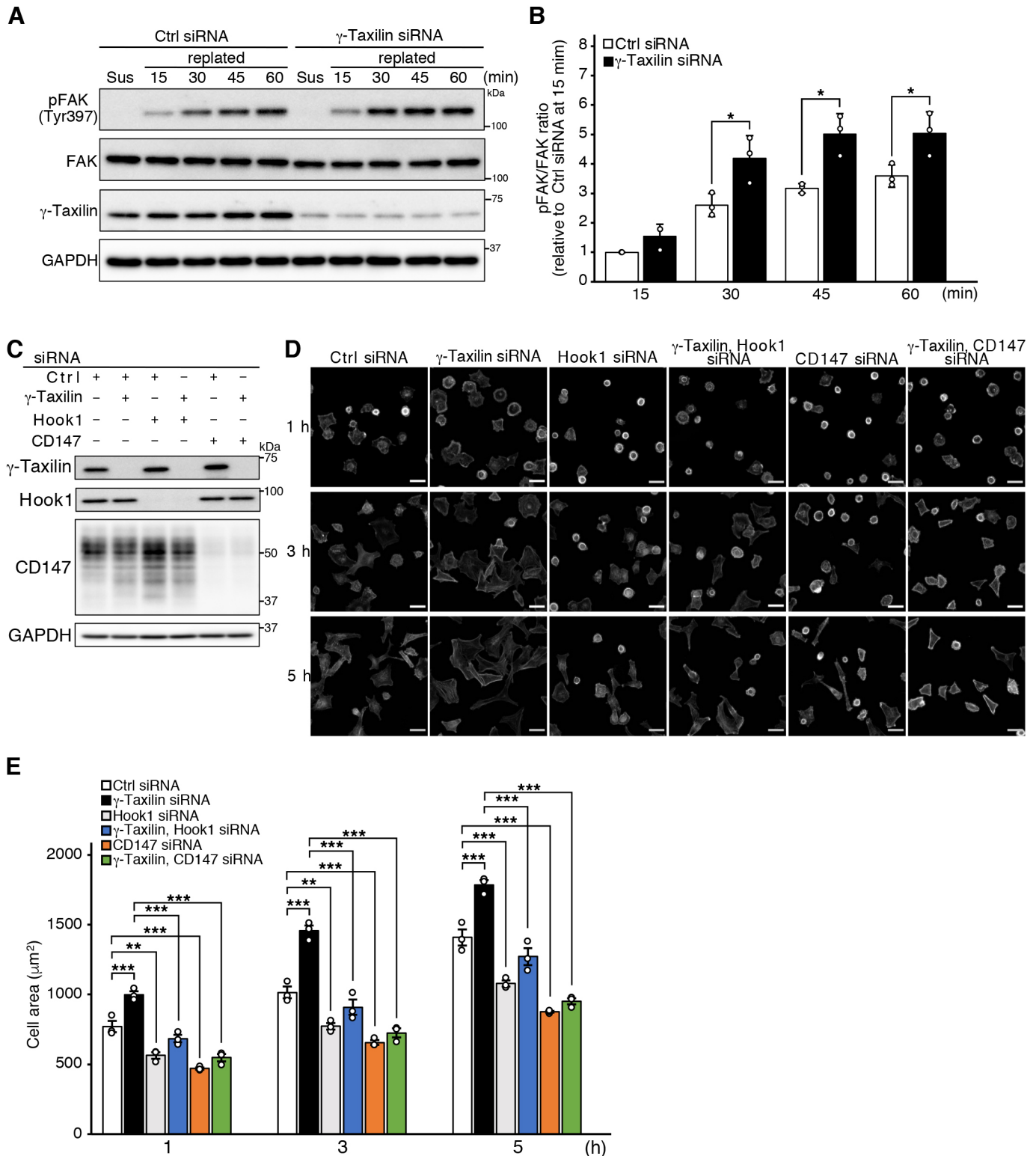


Fig. 6. γ -Taxilin depletion promotes cell spreading mediated by CD147. (A) Cell adhesion-dependent FAK-Tyr 397 phosphorylation. HeLa cells treated with the indicated siRNA were trypsinized and suspended in serum-free DMEM for 15 min. The suspended cells (Sus) were lysed or replated and then incubated for the indicated time periods. Cell lysates were subjected to SDS-PAGE followed by western blotting with the indicated antibodies. (B) Quantitative analysis of FAK-Tyr 397 phosphorylation in A. The results shown are the mean \pm s.d. of the ratio of pFAK to FAK relative to that with the Ctrl siRNA at time 15 min ($n=3$). * $P<0.05$ (two-tailed unpaired Student's t -test). (C) Co-depletion of γ -taxilin and Hook1 or CD147 by siRNA. Cells were transfected with control (Ctrl) or γ -taxilin (γ -taxilin #1) siRNA and Hook1 or CD147 siRNA. Cell lysates were subjected to SDS-PAGE followed by western blotting with the indicated antibodies. Blots are representative of three independent experiments. (D) Cell spreading assay. siRNA-treated HeLa cells were trypsinized and resuspended. The suspended cells were replated, incubated for the indicated time periods, and fixed. Cells were visualized using Alexa Fluor 594-labeled phalloidin. Scale bars: 40 μ m. (E) Quantitative analysis of cell spreading in D. The area of cell spreading at each time point was measured. Data are expressed as the mean \pm s.e.m. ($n=3$; >100 cells were analyzed in each experiment). ** $P<0.01$; *** $P<0.001$ (one-way ANOVA with post-hoc Tukey's multiple comparison test).

detection level, but hardly affected the expression levels of untargeted proteins (Fig. 6C). Unfortunately, we could not assess the recycling of CD147 to the plasma membrane because anti-CD147 antibody on the cell surface could not be removed by acid washing, but it is possible that γ -taxilin depletion promotes the recycling to the plasma membrane of not only CD98 but also CD147. Our results suggest that γ -taxilin depletion promotes spreading of HeLa cells by enhancing the Hook1-mediated recycling of CD147 to the plasma membrane, probably leading to the activation of β 1-integrin and FAK signaling.

γ -Taxilin binds to the C-terminal region of Hook1 competitively with CD98 and CD147

To test the possibility that γ -taxilin inhibits the Hook1-mediated biogenesis of tubular structures, we examined whether overexpression of γ -taxilin inhibits the formation of CD98-positive tubular structures. Overexpression of GFP- γ -taxilin, but not GFP, caused a significant decrease in the percentage of cells exhibiting CD98-positive tubular structures compared with control cells (Fig. 7A,B). CD98-positive tubular structures were prominently formed in GFP overexpressing cells rather than GFP- γ -taxilin overexpressing cells (Fig. 7A). The result raises the issue whether overexpression of γ -taxilin affects the subcellular localization of CD98 or not. It has been reported that Hook1 depletion exhibiting the effect on the formation of CD98-positive tubular structures similar to that of γ -taxilin overexpression redirects CD98 to the EEA1-positive endosomes from the tubules associated with recycling (Maldonado-Báez et al., 2013a). Then, we examined whether overexpression of γ -taxilin enhanced the co-localization of CD98 with EEA1-positive endosomes. CD98 was hardly co-localized with EEA1-positive endosomes in control cells (Fig. S7A,C). Overexpression of GFP- γ -taxilin, but not GFP, caused a significant increase in the co-localization of CD98 with EEA1-positive endosomes (Fig. S7A,C). When a similar experiment was performed using anti-CD147 antibody instead of anti-CD98 antibody, a similar result was obtained (Fig. S7B,C). Additionally, we examined using subcellular fractionation whether overexpression of γ -taxilin affects the subcellular localization of Hook1 or not. Hook1 was almost present in the cytosol fraction in control cells. Overexpression of either GFP or GFP- γ -taxilin did not affect the subcellular localization of Hook1 (Fig. S7D). These results prompted us to clarify how γ -taxilin affects the function of Hook1 in the formation of CD98-positive tubular structures. Hook1 has domain organization: N-terminal microtubule-binding, central coiled-coil clusters, and C-terminal organelle-binding (Lee et al., 2018). First, we examined which region of Hook1 is necessary for its interaction with γ -taxilin. When various myc-tagged Hook1 truncation mutants were co-expressed with HA- γ -taxilin in HeLa cells and the cell lysates were immunoprecipitated with an anti-myc antibody, HA- γ -taxilin was immunoprecipitated with myc-Hook1 (residues 1–728), myc-Hook1 (residues 167–728), and myc-Hook1 (residues 486–728), but not myc-Hook1 (residues 1–166) or myc-Hook1 (residues 1–485) (Fig. 7C,D). Consistent with the above result, when we performed a yeast two-hybrid screen using full-length γ -taxilin as bait, we captured a 603-nucleotide-long cDNA fragment encoding the C-terminal region of Hook1 (residues 528–728).

Next, we examined which region of Hook1 is necessary for its interaction with CD98, and whether CD98 interacts with γ -taxilin. When myc-Hook1 (residues 1–728) and myc-Hook1 (residues 486–728) were respectively co-expressed with Flag-CD98 in HeLa cells and the cell lysates were immunoprecipitated with an anti-Flag

antibody, both were immunoprecipitated with Flag-CD98 (Fig. 7E). When HA- γ -taxilin was co-expressed with Flag-CD98 in HeLa cells and the cell lysates were immunoprecipitated with an anti-Flag antibody, we were unable to detect HA- γ -taxilin co-immunoprecipitated with Flag-CD98 (Fig. 7F). These results indicate that γ -taxilin and CD98 bind to the same region of Hook1, suggesting the possibility that they competitively bind to Hook1.

Finally, to validate this possibility, we examined whether γ -taxilin interferes with the interaction between Hook1 and CD98 or CD147. When Flag-CD98 and myc-Hook1 were co-expressed with or without HA- γ -taxilin in HeLa cells and the cell lysates were immunoprecipitated with anti-Flag antibody, the amount of myc-Hook1 co-immunoprecipitated with Flag-CD98 was significantly reduced in the cells expressing HA- γ -taxilin compared with control cells (Fig. 7G). When a similar experiment was performed using pcDNA3-Flag-CD147 instead of pcDNA3-Flag-CD98, a similar result was obtained (Fig. S8). To further strengthen the possibility, we performed the competitive binding experiment using various amounts of pcDNA3-HA- γ -taxilin. The expression levels of HA- γ -taxilin were increased in a dose-dependent manner, but the expression levels of either Flag-CD98 or myc-Hook1 were not changed (Fig. 7H). The amounts of myc-Hook1 co-immunoprecipitated with Flag-CD98 were decreased in antiparallel with increasing expression levels of HA- γ -taxilin (Fig. 7H). Taken together, these results suggest that γ -taxilin interferes in the interaction of Hook1 with CD98 in the step where Hook1 recognizes and subsequently sorts CD98 to REs, leading to inhibition of the recycling of CD98 from sorting endosomes (SEs) to REs.

DISCUSSION

γ -Taxilin depletion enhanced the recycling to the plasma membrane of CD98 but not MHC-I or TfnR, a CME cargo protein. Because it is practically difficult to detect only CD147 recycled back to the plasma membrane, we failed to show the effect of γ -taxilin depletion on recycling of CD147 to the plasma membrane, but it is possible that γ -taxilin regulates the recycling of CD147 as well as CD98. In human hepatocellular carcinoma SMMC-7721 cells, both CD98 and CD147 participate in cell spreading through the activation of β 1-integrin and FAK signaling (Wu et al., 2015, 2016). However, in HeLa cells, as examined in the present study, CD147 depletion significantly inhibited cell spreading, but CD98 depletion hardly inhibited spreading, suggesting that CD147 but not CD98 is involved in spreading of HeLa cells. γ -Taxilin depletion prompted cell spreading, and the effects of γ -taxilin depletion on cell spreading were attenuated by co-depletion of CD147 or Hook1. Taken together with the result that γ -taxilin depletion promoted cell adhesion-dependent phosphorylation of FAK on Tyr397 downstream of integrin signaling, it is possible that γ -taxilin participates in cell spreading through the regulation of Hook1-mediated sorting of CD147 from SEs into REs, probably affecting the activity of CD147-associated integrin.

Increasing evidence has shown that distinct cytoplasmic sequences of cargo proteins are involved not only in their internalization into cells but also in their sorting in endosomes. It has been revealed that SNX27 associated with SNX-BAR, retromer, and WASP complex is involved in endosomal recycling of CME cargo proteins harboring a PDZ-interacting sequence such as β 2 adrenergic receptor, MCT1, and ATP7A (Lauffer et al., 2010; Steinberg et al., 2013; Temkin et al., 2011). Subsequently, it has been shown that the same SNX27 complex is also involved in endosomal recycling of CIE cargo proteins such as GLUT1

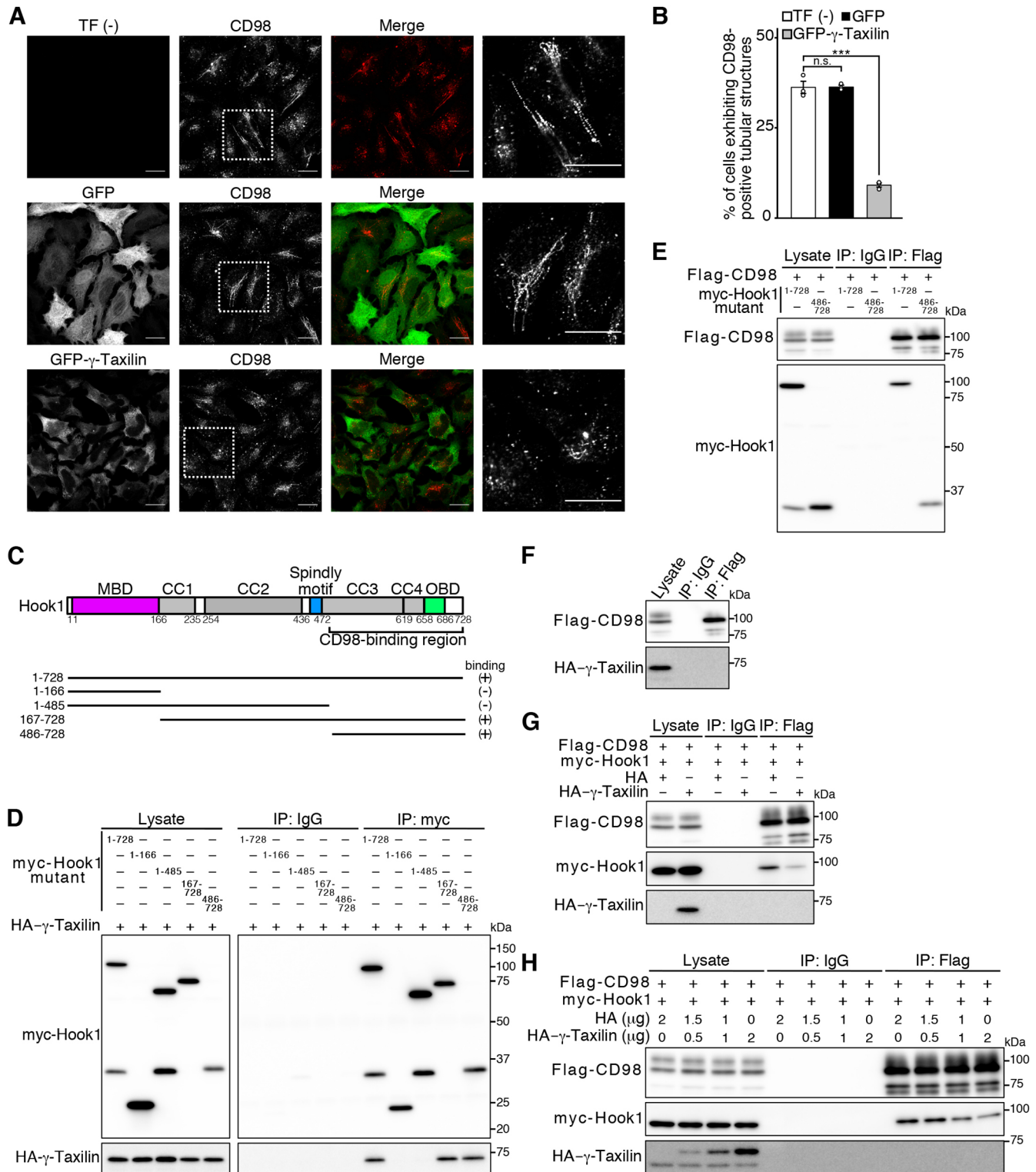


Fig. 7. γ -Taxilin binds to the C-terminal region of Hook1 competitively with CD98. (A) Formation of CD98-positive tubular structures in GFP- or GFP- γ -taxilin-expressing cells. Magnified views of the boxed areas in the panels of CD98 are shown in the right panels. Scale bars: 20 μ m. TF, transfection. (B) Quantitative analysis of the formation of CD98-positive tubular structures in A. Results shown are the mean \pm s.e.m. of the percentages of cells exhibiting CD98-positive tubular structures ($n=3$; >100 cells were analyzed in each experiment). *** $P<0.001$; n.s., not significant (one-way ANOVA with post-hoc Tukey's multiple comparison test). (C) Construction of myc-tagged Hook1 mutants used in D. MBD, microtubule-binding domain; CC, coiled-coil; OBD, organelle-binding domain. (D–H) Co-immunoprecipitation (IP) assays. Cells were co-transfected with the indicated plasmids. Cell lysates were immunoprecipitated with the indicated antibodies. The immunoprecipitates were subjected to SDS-PAGE followed by western blotting with the indicated antibodies for detection of the corresponding proteins ($n=3$, each experiment). (D) Analysis of the binding region of Hook1 necessary for interaction with γ -taxilin. (E) Analysis of the binding region of Hook1 for interaction with CD98. (F) Analysis of the interaction between γ -taxilin and CD98. (G) Analysis of competitive binding between γ -taxilin and CD98 to Hook1. (H) Dose-dependent effects of γ -taxilin on the interactions shown in G. The amount of cell lysates used for western blotting were 2.5% of those used for IP.

(encoded by *SLC2A1*) and CD147 (Steinberg et al., 2013) and that other distinct cytoplasmic sequences of CIE cargo proteins than PDZ-interacting sequence are involved in such sorting (Maldonado-Báez et al., 2013a). CIE cargo proteins entering cells through vesicular structures associated with Arf6 are at first transported to Rab5-positive EEs. From the endosomes, a group of CIE cargo proteins commonly harboring clusters of acidic amino acids in their cytoplasmic tail (CD44, CD147, and CD98) are directly transported to REs for recycling back to the plasma membrane, thus avoiding degradation in lysosomes, while another group of CIE cargo proteins not harboring the acidic clusters (MHC-I, CD55, and Tac) is transported to Rab5- and EEA1-positive endosomes via a default route, followed by transport to LEs and lysosomes for degradation, or to REs for recycling back to the plasma membrane (Maldonado-Báez et al., 2013a). It has been revealed that the binding of Hook1 through its C-terminal region to the acidic clusters of CD147 is involved in the sorting of CD147 from Rab5-positive EEs into REs (Maldonado-Báez et al., 2013a). The results of the present study strengthen the importance of the binding of Hook1 through its C-terminal region to the acidic clusters of CD98 and CD147 in the sorting of these endocytosed cargo proteins into REs.

We propose that γ -taxilin works at the initiation step where Hook1 recognizes and directly sorts CIE cargo proteins from SEs into REs (Fig. 8). Two other proteins that interact with the C-terminal region of Hook1, the Vps18 subunit of the homotypic vesicular protein sorting (HOPS) complex and AKT-interacting protein (AKTIP), an E2 ubiquitin-conjugating enzyme also known as fused toes (FTS), have been identified (Richardson et al., 2004; Xu et al., 2008). However, our present findings provide the first evidence that a Hook1-interacting protein plays a role in sorting of CIE cargo proteins into REs. We do not know whether γ -taxilin affects the interaction of Hook1 with Vps18 or AKTIP in the sorting step from EEs to LEs and lysosomes. Further studies are necessary to evaluate the possibility that γ -taxilin is involved in trafficking of endocytosed cargo proteins from EEs to LEs and lysosomes.

Rab proteins are key regulators in various steps of the endocytic pathway (Zhen and Stenmark, 2015) and increasing evidence has shown that several Rab proteins participate in RE dynamics. Rab10, Rab11, and Rab22a are involved in the formation of KIF13A-positive tubular REs; KIF13A is an RE marker (Delevoeye et al., 2014; Etoh and Fukuda, 2019; Patel et al., 2021). Rab10 and Rab35 participate in the formation of MICAL-L1-positive tubular structures (Etoh and Fukuda, 2019; Rahajeng et al., 2012). It has been revealed that Rab22a is involved in sorting of CD98 and CD147 from SEs into REs (Maldonado-Báez et al., 2013a). Overexpression of Rab22a restores the formation of CD147-positive tubular structures in cells expressing a dominant-negative mutant of Hook1 in which the formation of CD147-positive tubular structures is decreased. Conversely, Hook1 overexpression restores the formation of CD147-positive tubular structures in cells expressing a dominant-negative mutant of Rab22a in which the formation of CD147-positive tubular structures is decreased (Maldonado-Báez et al., 2013a). On the basis of the reciprocal rescue of their respective dominant-negative phenotypes, it has been proposed that Rab22a works co-operatively with Hook1 in the same step of recycling of CIE cargo proteins back to the plasma membrane (Maldonado-Báez et al., 2013a). Our present result that simultaneous depletion of Rab22a and γ -taxilin attenuated the effect of γ -taxilin depletion on the formation of CD98-positive tubular structures supports our proposal that γ -taxilin negatively regulates the Hook1-mediated sorting of endocytosed CIE cargo proteins into REs. The formation of MHC-I-positive tubular structures in cells expressing dominant-negative and dominant-active mutants of Rab22a is inhibited and enhanced, respectively, and both mutants inhibit recycling of MHC-I to the plasma membrane (Weigert et al., 2004). As in addition to larger MHC-I-positive tubular structures, MHC-I-positive vesicles at the cell periphery are observed in cells expressing the dominant-active mutant of Rab22a, it is thought that Rab22a cycling between GTP-bound active and GDP-bound inactive states is required for recycling of MHC-I from SEs to the plasma membrane (Weigert et al., 2004). CD98-positive peripheral vesicles similar to the MHC-I-positive peripheral vesicles in cells expressing

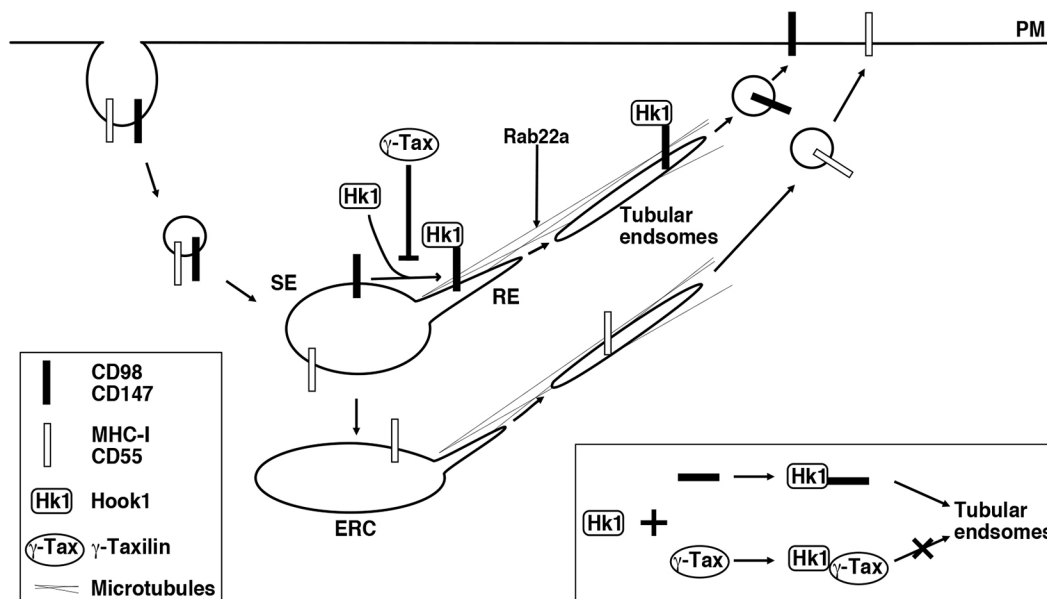


Fig. 8. The proposed role of γ -taxilin in recycling of clathrin-independent cargo. γ -Taxilin functions, at least, in the step where Hook1 recognizes and subsequently sorts Hook1-mediated cargo proteins such as CD98 and CD147 from sorting endosomes to recycling endosomes, forming tubular structures. γ -Taxilin interferes with the interaction between Hook1 and Hook1-mediated cargo proteins, leading to inhibition of the recycling of these cargo proteins back to the plasma membrane. ERC, endocytic recycling compartment; PM, plasma membrane; RE, recycling endosome; SE, sorting endosome.

the dominant-active mutant of Rab22a were not observed in γ -taxilin-depleted cells. Therefore, it is unlikely that γ -taxilin depletion inhibits the fusion of Hook1-mediated CIE cargo protein-loaded vesicles with the plasma membrane. On the other hand, our present result that simultaneous depletion of Rab10 with γ -taxilin attenuates the effect of γ -taxilin depletion on the formation of CD98-positive tubular structures raises the possibility that Rab10 is also involved in the formation and maintenance of Hook1-associated CIE cargo protein-positive tubular structures.

Nakamura and colleagues have shown that γ -taxilin is involved in hypoxia-induced ER stress responses in a GSK-3 β -dependent manner (Hotokezaka et al., 2015). We do not know whether the ER stress responses induced by depletion of γ -taxilin indirectly participate in the regulation of the Hook1-mediated endocytic pathway, but it seems unlikely, as γ -taxilin depletion was reported to induce ER stress responses followed by apoptosis in HeLa S3 cells 72–96 h after transfection but all our experiments were performed at earlier time points. Taken together with the evidence that CD147, a subunit of γ -secretase, is involved in the production of amyloid- β related to the pathogenesis of Alzheimer's disease (AD) (Zhou et al., 2005), the finding that the expression level of γ -taxilin is decreased not only in mouse brain slices cultured in hypoxic conditions but also in the brain of patients with AD (Hotokezaka et al., 2015) suggests that γ -taxilin might be implicated in the pathology of AD by affecting the recycling of CD147 to the plasma membrane as well as its involvement in ER stress responses. St-Arnaud and colleagues have shown that γ -taxilin present in the nucleus inhibits the transcriptional activity of ATF4, inducing the differentiation of osteoblasts (Yu et al., 2005, 2008). We have shown that γ -taxilin localized to centrosomes temporally regulates centrosome disjunction in a Nek2A-dependent manner (Makiyama et al., 2018). Moreover, our finding suggesting the interaction of γ -taxilin with Hook2, which is localized to centrosomes, implies an unraveled function of γ -taxilin in centrosomes. Thus, accumulating evidence strongly supports that γ -taxilin has diverse functions, and it is important to comprehensively reveal the relationships between these functions.

CD98 and CD147, which are directly sorted from SEs into REs by Hook1, are implicated in various physiological and pathological processes. CD147 is involved in lymphocyte responsiveness, spermatogenesis, implantation, fertilization, and neurological functions, and pathology including rheumatoid arthritis, atherosclerosis, and tumor metastasis (Muramatsu, 2016). CD98 and CD147 on the cell surface associate with and regulate the activities of various proteins such as transporters, integrins, and matrix metalloproteinases (Muramatsu, 2016). On the basis of our present findings suggesting that γ -taxilin modulates the number of CD98 and CD147 molecules residing on the cell surface by regulating their recycling back from SEs to the plasma membrane, it is possible that γ -taxilin is involved in these CD98- and CD147-related physiological and pathological processes. In our current model (Fig. 8), the molecular mechanism by which the interaction between γ -taxilin and Hook1 is regulated is not clear. However, because it has been reported that Arf6 is involved in HGF-induced cell spreading (Hongu et al., 2015) and that Arf6 participates in endocytic recycling of CD147 (Qi et al., 2019), it is possible that the interaction between γ -taxilin and Hook1 might be regulated by the Arf6-related pathway. Furthermore, phosphorylation on several predicted phosphorylation sites of γ -taxilin, which are reported by PhosphoSitePlus (<http://www.phosphosite.org>), might be involved in the above putative regulation pathway.

In conclusion, our study uncovers a novel molecular mechanism underlying the regulation of CIE, which at least sheds light on the

mode of activation of CD98 and CD147. Taken together with our previous reports (Sakane et al., 2014, 2016), our present findings at least suggest that taxilin family members could be commonly involved in the sorting of various endocytosed cargo proteins on SEs.

MATERIALS AND METHODS

Antibodies

An anti- γ -taxilin antibody (80 ng/ml for western blotting and 1 μ g/20 μ l beads for immunoprecipitation) was prepared as described previously (Nogami et al., 2004). An anti-Hook1 antibody (ab151756; 1:1000 for western blotting and 1:100 for immunocytochemistry) was purchased from Abcam. Anti-CD55 (311302; 1:100 for antibody uptake assay), anti-CD98 (315602; 1:100 for antibody uptake assay, recycling assay, and internalization assay), anti-CD147 (306202; 1:100 for antibody uptake assay), and anti-MHC-I (311402; 1:100 for antibody uptake assay and recycling assay) antibodies were purchased from BioLegend. Anti-CD98 (15193-1-AP; 1:5000 for western blotting) and anti-Rab22a (12125-1-AP; 1:1000 for western blotting) antibodies were purchased from Proteintech. Anti-CD147 (34-5600; 1:125 for western blotting) and anti-TfnR (13-6800; 1:1000 for western blotting) antibodies were purchased from Invitrogen. Anti-EEA1 (2411; 1:100 for immunocytochemistry), anti-FAK (3285; 1:1000 for western blotting), anti-pFAK (Tyr397) (3283; 1:1000 for western blotting), and anti-Rab10 (8127; 1:1000 for western blotting) antibodies were purchased from Cell Signaling Technology. Anti- α -tubulin (T9026; 1:5000 for western blotting) and anti- γ -taxilin (HPA000841; 1:200 for immunocytochemistry) antibodies were purchased from Sigma-Aldrich. Anti-GAPDH (M171-3; 1:4000 for western blotting), anti-HA (561; 1:1000 for western blotting), anti-myc (562; 1:1000 for western blotting), anti-Flag (M185; 1:10,000 for western blotting) antibodies, mouse IgG2a (M076-3), and rabbit IgG (PM035) were purchased from MBL. Horseradish peroxidase- and Alexa Fluor-conjugated secondary antibodies were purchased from GE Healthcare and Thermo Fisher Scientific, respectively.

DNA constructs

pGBKT7- α -, β -, and γ -taxilin and pEGFPC1- γ -taxilin were constructed as described previously (Makiyama et al., 2018; Sakane et al., 2016). Full-length human α -, β -, and γ -taxilin cDNA fragments were amplified from pGBKT7- α - and β -taxilin, and pEGFPC1- γ -taxilin, respectively, by PCR. The full-length human α - and β -taxilin cDNA fragments were introduced into the *EcoRI* and *BamHI* site of pcDNA3-HA using an In-Fusion HD Cloning Kit (Clontech, Takara Bio). The full-length human γ -taxilin cDNA fragment was introduced into the *EcoRV* site of pcDNA3-HA using the same kit. For generating siRNA-resistant γ -taxilin expression plasmid (pEGFPC1- γ -taxilin-mt), five silent substitutions were introduced in the region complementary to γ -taxilin #1 siRNA using the PrimeSTAR Mutagenesis Basal Kit (Takara Bio) according to the manufacturer's protocol. Full-length cDNA fragments encoding human Hook1, Hook2, and Hook3, human CD98, and human CD147 were amplified by PCR from HeLa cDNA. The full-length human Hook1 and Hook2 cDNA fragments were introduced into the *EcoRI* and *XhoI* sites of vectors pGADT7 and pcDNA3-myc. The full-length human Hook3 cDNA fragment was introduced into the *EcoRI* and *Clal* sites of pGADT7 and the *EcoRI* and *XhoI* sites of pcDNA3-myc. pcDNA3-myc-Hook1 (residues 1–485), pcDNA3-myc-Hook1 (residues 1–166), pcDNA3-myc-Hook1 (residues 167–728), and pcDNA3-myc-Hook1 (residues 486–728) were constructed from pcDNA3-myc-Hook1 using the PrimeSTAR Mutagenesis Basal Kit (Takara Bio) according to the manufacturer's protocol. The full-length human CD98 and CD147 cDNA fragments were introduced into the *BamHI* and *EcoRI* sites of pcDNA3-C-terminal Flag. The PCR products and the structures of all plasmids were confirmed by DNA sequencing.

Cell culture and transfection

HeLa cells were grown in Dulbecco's modified Eagle's medium (DMEM) high glucose (Wako) with 10% fetal bovine serum, 2 mM glutamine, 100 U/ml penicillin, and 0.1 mg/ml streptomycin (referred to hereafter as complete DMEM) in a 5% CO₂ incubator at 37°C. Transfection of plasmid DNA and

siRNA into cells was performed using Lipofectamine 2000 and Lipofectamine RNAiMAX (Thermo Fisher Scientific), respectively, according to the manufacturer's protocols. Lipofectamine 2000- and Lipofectamine RNAiMAX-treated cells were, respectively, used for experiments 24 and 48 h post-transfection. For siRNA rescue experiments, γ -taxilin siRNA-treated cells were transfected with pEGFPC1- γ -taxilin-mt or pEGFPC1- γ -taxilin at 24 h after treatment with γ -taxilin siRNA. After incubation for 24 h, cells were processed for the experiments. Silencer Select negative control siRNA (4390843) and Silencer Select siRNAs against γ -taxilin#1 (ID s31509), γ -taxilin#2 (ID s31511), Hook1 (ID s28011), CD98 (ID s12943), CD147 (ID s2099), Rab10 (ID s21390), and Rab22a (ID s32992) were purchased from Thermo Fisher Scientific.

Yeast two-hybrid assay

Yeast two-hybrid assays were performed using the Matchmaker Gold Yeast Two-Hybrid System (Takara Bio) according to the manufacturer's protocol. pGBKT7- γ -taxilin was introduced into yeast strain Y2H Gold, and the transformant was mated with yeast strain Y187 harboring a human normalized cDNA library (Clontech, Takara Bio). Library plasmids from positive clones were analyzed by transformation tests and DNA sequencing. BLAST searches were conducted using the NCBI online service. To examine the interaction of Hook1, Hook2, or Hook3 with α -, β -, or γ -taxilin, a pGADT7-based vector harboring a Hook1, Hook2, or Hook3 cDNA fragment and a pGBKT7-based vector harboring an α -, β -, or γ -taxilin cDNA fragment were introduced into strain Y2H Gold. Equal amounts of the transformants were spotted on to synthetic medium lacking leucine, tryptophan, and histidine with 10 mM 3-amino-1,2,4-triazole (Tokyo Kasei Kogyo) (–LWH plates) to examine the interaction between co-expressed proteins, or on to synthetic medium lacking leucine and tryptophan (–LW plates) to examine plasmid maintenance, and then incubated for 3 days at 30°C.

Western blotting

Cells were lysed in lysis buffer [20 mM Tris-HCl (pH 8.0), 150 mM NaCl, 1% Nonidet P-40, 10% glycerol, and protease inhibitor cocktail (Roche Diagnostics)]. Protein concentration was determined using a DC Protein Assay Kit (Bio-Rad). Cell lysates were subjected to SDS-PAGE followed by western blotting. Immunoreactive bands were detected using the ECL Prime Western Blotting Detection Reagent (GE Healthcare), Clarity Western ECL substrate (Bio-Rad), or SuperSignal West Atto Ultimate Sensitivity Substrate (Thermo Fisher Scientific) and captured using an Amersham Imager 600 (Amersham). Band intensities were measured using the Fiji package of ImageJ software (NIH).

Immunoprecipitation

Transfected HeLa cells were lysed in immunoprecipitation buffer (20 mM HEPES-NaOH, pH 7.0, 150 mM NaCl, 0.1% Triton X-100, 10% glycerol, and protease inhibitor cocktail) and then 250 μ l of the cell lysate (0.3 mg protein) was immunoprecipitated with 2 μ g of mouse IgG2a, rabbit IgG, or anti-HA, anti-myc, or anti-flag antibody overnight at 4°C. The immunoprecipitates were collected with 20 μ l of Protein G–Sepharose (GE Healthcare), washed five times with lysis buffer, and used for western blotting. The secondary antibody used for western blot analysis was TidyBlot Western Blot Detection Reagent (Bio-Rad). For analysis of endogenous protein interactions, HeLa cells were lysed in immunoprecipitation buffer and then 1 ml of the cell lysate (1 mg of protein) was immunoprecipitated with 1 μ g of rabbit IgG or anti- γ -taxilin antibody overnight at 4°C. The following steps were performed as described above and immunoreactive bands were detected using SuperSignal West Atto Ultimate Sensitivity Substrate (Thermo Fisher Scientific).

Immunocytochemistry

Cells grown on glass coverslips were fixed in PBS containing 2% paraformaldehyde (PFA) for 10 min and stained with primary antibody in PBS containing 0.5% bovine serum albumin (BSA) and 0.2% saponin for 1 h at room temperature. After washing three times with PBS, the cells were

treated with the secondary antibody in PBS containing 0.5% BSA and 0.2% saponin for 1 h at room temperature. Cells were observed using a confocal laser scanning microscope (LSM 710, Carl Zeiss).

Antibody uptake assay

Cells grown on glass coverslips were incubated with primary antibodies against CIE cargo proteins (CD55, CD98, CD147, or MHC-I) for 1 h at 37°C to allow internalization of the antibody-bound CIE cargo proteins. The following procedures were performed at room temperature. In the case of CD98 and MHC-I, cells were treated with low pH solution (0.5% acetic acid, 0.5 M NaCl) for 30 s to remove surface-bound antibody before fixation with 2% PFA in PBS for 10 min. In the case of CD55 and CD147, cells were treated with unlabeled anti-mouse IgG (Jackson ImmunoResearch Laboratories) for 1 h to block surface-bound antibodies after the same fixation. Internalized antibodies were detected by incubating cells with Alexa Fluor-conjugated secondary antibody in PBS containing 5% BSA and 0.1% saponin for 1 h. Cells were observed using a confocal laser scanning microscope (LSM 710, Carl Zeiss). Cells containing at least one tubule >5 μ m long were counted as exhibiting tubular structures.

Time-lapse imaging

A CD98 antibody was labeled for fluorescence detection using an Alexa Fluor 488 Antibody Labeling Kit (Thermo Fisher Scientific) according to the manufacturer's protocol. Cells grown on glass-bottomed dishes were incubated with the Alexa Fluor 488-labeled anti-CD98 antibody for 1 h at 37°C. After washing twice with complete DMEM, the cells were further incubated in complete DMEM to analyze internalized Alexa Fluor 488-labeled anti-CD98 antibody by live-cell imaging using an inverted fluorescence microscope (Axio Observer Z1, Carl Zeiss). During live-cell imaging, cells were maintained in a 5% CO₂ stage top incubator with an objective heater (Tokai Hit) at 37°C. Time-lapse images were captured at 10-s intervals over 10 min. Because CD98-positive tubules are highly dynamic structures that frequently extend, retract, and branch, CD98-positive tubules newly formed during the period of observation, but not pre-formed CD98-positive tubules, were analyzed. When the newly formed CD98-positive tubules branched, the branched CD98-positive tubule was analyzed as another newly formed CD98-positive tubule. The number and length of newly formed CD98-positive tubules during the period of observation were counted and manually measured, respectively. The number and the length of newly formed tubules were evaluated independently by three of the authors. Newly formed CD98-positive tubules were categorized into five groups (<5 μ m, 5–10 μ m, 11–15 μ m, 16–20 μ m, and >20 μ m) by the maximum length of the newly formed CD98-positive tubule.

Internalization assay

Cells grown on glass coverslips were incubated with anti-CD98 antibody in DMEM containing 0.5% BSA for 1 h at 4°C. The cells were washed twice with PBS, followed by two rinses with DMEM. Then, the cells were further incubated for various time periods in complete DMEM at 37°C. In the case of detection of surface-bound anti-CD98 antibody at time zero, cells were fixed and stained without permeabilization. In the case of detection of internalized anti-CD98 antibody, the cells were treated with the low pH solution to remove surface-bound anti-CD98 antibody. Then, the cells were fixed, permeabilized, and stained. Cells were observed using a confocal laser scanning microscope (LSM 710, Carl Zeiss). The signal intensities of intracellular and surface anti-CD98 per μ m² were measured using ZEN (blue edition) software (Carl Zeiss).

Recycling assay

In the case of CD98 and MHC-I, cells grown on glass coverslips were incubated with anti-CD98 or anti-MHC-I antibody for 1 h at 37°C. After incubation, the cells were treated with the low pH solution to remove surface-bound antibodies, followed by two rinses with PBS and two rinses with complete DMEM. The cells were further incubated in complete DMEM for various time periods at 37°C. The following procedures were

performed at room temperature. In the case of detection of intracellular antibodies, cells were treated with the low pH solution to remove antibody recycled back to the surface membrane. Then, the cells were fixed in PBS containing 2% PFA for 10 min and stained with Alexa Fluor-conjugated secondary antibody in PBS containing 5% BSA and 0.1% saponin. In the case of detection of antibodies recycled back to the surface membrane, cells were fixed and stained without permeabilization. In the case of TfnR, cells grown on glass coverslips were serum-starved for 30 min at 37°C and then incubated with Tfn-594 (Thermo Fisher Scientific) for 1 h at 37°C. Then, the cells were treated with the low pH solution to remove cell surface Tfn-594, followed by two rinses with PBS and two rinses with complete DMEM. The cells were further incubated for various time periods at 37°C in complete DMEM, subsequently washed twice with PBS, and fixed at room temperature. Cells were observed using a confocal laser scanning microscope (LSM 710, Carl Zeiss). The signal intensities of intracellular and cell surface antibodies and intracellular Tfn-594 per μm^2 were measured using ZEN (blue edition) software.

FAK signaling analysis

For analysis of basal phosphorylation of FAK on Tyr397, cells were lysed in lysis buffer containing phosphatase inhibitor cocktail (524625, Merck). For analysis of cell adhesion-dependent phosphorylation of FAK on Tyr397, cells were trypsinized, neutralized by addition of PBS containing 0.25% soybean trypsin inhibitor, washed twice with DMEM by centrifugation, and resuspended in DMEM. After incubation for 15 min at 37°C, the suspended cells were seeded on culture dishes and further cultured in complete DMEM for various time periods at 37°C. Replated cells were lysed in lysis buffer containing phosphatase inhibitor cocktail. Cell lysates were processed for western blotting as described above.

Cell spreading assay

Cells were trypsinized, washed once with complete DMEM by centrifugation to neutralize the trypsin, and resuspended in complete DMEM. The suspended cells were seeded on glass coverslips and cultured in complete DMEM for various time periods at 37°C. The cells were fixed in PBS containing 2% PFA for 10 min and stained with Alexa Fluor 594-conjugated phalloidin (Thermo Fisher Scientific). Cells were observed using an inverted fluorescence microscope (Axio Observer Z1, Carl Zeiss). The cell area was measured using the Fiji package of ImageJ.

Subcellular fractionation

Subcellular fractionation was performed using the SF PTS Kit (7510-11400, GL Sciences) according to the manufacturer's protocol.

Statistical analysis

All statistical analyses were performed using IBM SPSS Statistics version 26 software. Results are presented as means \pm s.d. or s.e.m. $P < 0.05$ was considered statistically significant.

Acknowledgements

We thank T. Namatame, Clinical Research Center, Dokkyo Medical University, for DNA sequencing and Ms M. Ooshima and A. Akima for technical assistance and secretarial assistance. We thank James Allen, DPhil, from Edanz Group (<https://en-author-services.edanz.com/ac>) for editing a draft of the manuscript.

Competing interests

The authors declare no competing or financial interests.

Author contributions

Conceptualization: S.H., H. Shirataki; Methodology: S.H., T.M.; Formal analysis: S.H., T.M., H. Shirataki; Investigation: S.H.; Resources: S.H., T.M., H. Sakane, S.N., H. Shirataki; Writing - original draft: S.H., H. Shirataki; Writing - review & editing: S.H., S.N., H. Shirataki; Visualization: S.H.; Supervision: H. Shirataki; Project administration: H. Shirataki; Funding acquisition: S.H.

Funding

This work was supported in part by Japan Society for the Promotion of Science KAKENHI (grant number 19K17045 to S.H.).

Peer review history

The peer review history is available online at <https://journals.biologists.com/jcs/article-lookup/doi/10.1242/jcs.258849>.

References

- Baron Gaillard, C. L., Pallesi-Pocachard, E., Massey-Harroche, D., Richard, F., Arsanto, J.-P., Chauvin, J. P., Lecine, P., Krämer, H., Borg, J.-P. and Le Bivic, A. (2011). Hook2 is involved in the morphogenesis of the primary cilium. *Mol. Biol. Cell* **22**, 4549-4562. doi:10.1091/mbc.e11-05-0405
- Del Olmo, T., Lauzier, A., Normandin, C., Larcher, R., Lecours, M., Jean, D., Lessard, L., Steinberg, F., Boisvert, F. M. and Jean, S. (2019). APEX2-mediated RAB proximity labeling identifies a role for RAB21 in clathrin-independent cargo sorting. *EMBO Rep.* **20**, e47192. doi:10.15252/embr.201847192
- Delevoeye, C., Miserey-Lenkei, S., Montagnac, G., Gilles-Marsens, F., Paul-Gilloteaux, P., Giordano, F., Waharte, F., Marks, M. S., Goud, B. and Raposo, G. (2014). Recycling endosome tubule morphogenesis from sorting endosomes requires the kinesin motor KIF13A. *Cell Rep.* **6**, 445-454. doi:10.1016/j.celrep.2014.01.002
- Dutta, D. and Donaldson, J. G. (2015). Sorting of clathrin-independent cargo proteins depends on Rab35 delivered by clathrin-mediated endocytosis. *Traffic* **16**, 994-1009. doi:10.1111/tra.12302
- Etoh, K. and Fukuda, M. (2019). Rab10 regulates tubular endosome formation through KIF13A and KIF13B motors. *J. Cell Sci.* **132**, jcs226977. doi:10.1242/jcs.226977
- Grant, B. D. and Donaldson, J. G. (2009). Pathways and mechanisms of endocytic recycling. *Nat. Rev. Mol. Cell Biol.* **10**, 597-608. doi:10.1038/nrm2755
- Hoffmann, J., Boehm, C., Himmelsbach, K., Donnerhak, C., Roettger, H., Weiss, T. S., Ploen, D. and Hildt, E. (2013). Identification of α -taxilin as an essential factor for the life cycle of hepatitis B virus. *J. Hepatol.* **59**, 934-941. doi:10.1016/j.jhep.2013.06.020
- Hongu, T., Funakoshi, Y., Fukuhara, S., Suzuki, T., Sakimoto, S., Takakura, N., Ema, M., Takahashi, S., Itoh, S., Kato, M. et al. (2015). Arf6 regulates tumour angiogenesis and growth through HGF-induced endothelial β 1 integrin recycling. *Nat. Commun.* **6**, 7925. doi:10.1038/ncomms8925
- Horii, Y., Sakane, H., Nogami, S., Ohtomo, N., Tomiya, T. and Shirataki, H. (2014). Expression of α -taxilin in the murine gastrointestinal tract: potential implication in cell proliferation. *Histochem. Cell Biol.* **141**, 165-180. doi:10.1007/s00418-013-1147-0
- Hotokezaka, Y., Katayama, I., van Leyen, K. and Nakamura, T. (2015). GSK-3 β -dependent downregulation of γ -taxilin and α NAC merge to regulate ER stress responses. *Cell Death Dis.* **6**, e1719. doi:10.1038/cddis.2015.90
- Huveneers, S. and Danen, E. H. J. (2009). Adhesion signaling - crosstalk between integrins, Src and Rho. *J. Cell Sci.* **122**, 1059-1069. doi:10.1242/jcs.039446
- Krämer, H. and Phistry, M. (1996). Mutations in the Drosophila hook gene inhibit endocytosis of the boss transmembrane ligand into multivesicular bodies. *J. Cell Biol.* **133**, 1205-1215. doi:10.1083/jcb.133.6.1205
- Krämer, H. and Phistry, M. (1999). Genetic analysis of hook, a gene required for endocytic trafficking in drosophila. *Genetics* **151**, 675-684. doi:10.1093/genetics/151.2.675
- Lauffer, B. E. L., Melero, C., Temkin, P., Lei, C., Hong, W., Kortemme, T. and von Zastrow, M. (2010). SNX27 mediates PDZ-directed sorting from endosomes to the plasma membrane. *J. Cell Biol.* **190**, 565-574. doi:10.1083/jcb.201004060
- Lee, I.-G., Olenick, M. A., Boczkowska, M., Franzini-Armstrong, C., Holzbaur, E. L. F. and Dominguez, R. (2018). A conserved interaction of the dynein light intermediate chain with dynein-dynactin effectors necessary for processivity. *Nat. Commun.* **9**, 986. doi:10.1038/s41467-018-03412-8
- Makiyama, T., Higashi, S., Sakane, H., Nogami, S. and Shirataki, H. (2018). γ -Taxilin temporally regulates centrosome disjunction in a Nek2A-dependent manner. *Exp. Cell Res.* **362**, 412-423. doi:10.1016/j.yexcr.2017.12.004
- Maldonado-Báez, L., Cole, N. B., Krämer, H. and Donaldson, J. G. (2013a). Microtubule-dependent endosomal sorting of clathrin-independent cargo by Hook1. *J. Cell Biol.* **201**, 233-247. doi:10.1083/jcb.201208172
- Maldonado-Báez, L., Williamson, C. and Donaldson, J. G. (2013b). Clathrin-independent endocytosis: a cargo-centric view. *Exp. Cell Res.* **319**, 2759-2769. doi:10.1016/j.yexcr.2013.08.008
- Mashidori, T., Shirataki, H., Kamai, T., Nakamura, F. and Yoshida, K.-I. (2011). Increased alpha-taxilin protein expression is associated with the metastatic and invasive potential of renal cell cancer. *Biomed. Res.* **32**, 103-110. doi:10.2220/biomedres.32.103
- Mayor, S., Parton, R. G. and Donaldson, J. G. (2014). Clathrin-independent pathways of endocytosis. *Cold Spring Harb. Perspect Biol.* **6**, a016758. doi:10.1101/cshperspect.a016758
- Mendoza-Lujambio, I., Burfeind, P., Dixkens, C., Meinhardt, A., Hoyer-Fender, S., Engel, W. and Neesen, J. (2002). The Hook1 gene is non-functional in the abnormal spermatozoon head shape (azh) mutant mouse. *Hum. Mol. Genet.* **11**, 1647-1658. doi:10.1093/hmg/11.14.1647

- Muramatsu, T.** (2016). Basigin (CD147), a multifunctional transmembrane glycoprotein with various binding partners. *J. Biochem.* **159**, 481–490. doi:10.1093/jb/mvv127
- Nogami, S., Satoh, S., Nakano, M., Shimizu, H., Fukushima, H., Maruyama, A., Terano, A. and Shirataki, H.** (2003). Taxilin: a novel syntaxin-binding protein that is involved in Ca²⁺-dependent exocytosis in neuroendocrine cells. *Genes Cells* **8**, 17–28. doi:10.1046/j.1365-2443.2003.00612.x
- Nogami, S., Satoh, S., Tanaka-Nakadate, S., Yoshida, K., Nakano, M., Terano, A. and Shirataki, H.** (2004). Identification and characterization of taxilin isoforms. *Biochem. Biophys. Res. Commun.* **319**, 936–943. doi:10.1016/j.bbrc.2004.05.073
- Oba-Shinjo, S. M., Bengtson, M. H., Winnischofer, S. M. B., Colin, C., Vedoy, C. G., de Mendonça, Z., Marie, S. K. N. and Sogayar, M. C.** (2005). Identification of novel differentially expressed genes in human astrocytomas by cDNA representational difference analysis. *Brain Res. Mol. Brain Res.* **140**, 25–33. doi:10.1016/j.molbrainres.2005.06.015
- Ohtomo, N., Tomiya, T., Tanoue, Y., Inoue, Y., Nishikawa, T., Ikeda, H., Seyama, Y., Kokudo, N., Shibahara, J., Fukayama, M. et al.** (2010). Expression of α -taxilin in hepatocellular carcinoma correlates with growth activity and malignant potential of the tumor. *Int. J. Oncol.* **37**, 1417–1423. doi:10.3892/ijco.00000793
- Patel, N. M., Siva, M. S. A., Kumari, R., Shewale, D. J., Rai, A., Ritt, M., Sharma, P., Setty, S. R. G., Sivaramakrishnan, S. and Soppina, V.** (2021). KIF13A motors are regulated by Rab22A to function as weak dimers inside the cell. *Sci. Adv.* **7**, eabd2054. doi:10.1126/sciadv.abd2054
- Qi, S., Su, L., Li, J., Zhang, C., Ma, Z., Liu, G., Zhang, Q., Jia, G., Piao, Y. and Zhang, S.** (2019). Arf6-driven endocytic recycling of CD147 determines HCC malignant phenotypes. *J. Exp. Clin. Cancer Res.* **38**, 471. doi:10.1186/s13046-019-1464-9
- Rahajeng, J., Giridharan, S. S., Cai, B., Naslavsky, N. and Caplan, S.** (2012). MICAL-L1 is a tubular endosomal membrane hub that connects Rab35 and Arf6 with Rab8a. *Traffic* **13**, 82–93. doi:10.1111/j.1600-0854.2011.01294.x
- Richardson, S. C. W., Winistorfer, S. C., Poupon, V., Luzio, J. P. and Piper, R. C.** (2004). Mammalian late vacuole protein sorting orthologues participate in early endosomal fusion and interact with the cytoskeleton. *Mol. Biol. Cell* **15**, 1197–1210. doi:10.1091/mbc.e03-06-0358
- Sakane, H., Horii, Y., Nogami, S., Kawano, Y., Kaneko-Kawano, T. and Shirataki, H.** (2014). α -Taxilin interacts with sorting nexin 4 and participates in the recycling pathway of transferrin receptor. *PLoS ONE* **9**, e93509. doi:10.1371/journal.pone.0093509
- Sakane, H., Makiyama, T., Nogami, S., Horii, Y., Akasaki, K. and Shirataki, H.** (2016). β -Taxilin participates in differentiation of C2C12 myoblasts into myotubes. *Exp. Cell Res.* **345**, 230–238. doi:10.1016/j.yexcr.2016.05.016
- Sharma, M., Giridharan, S. S. P., Rahajeng, J., Naslavsky, N. and Caplan, S.** (2009). MICAL-L1 links EHD1 to tubular recycling endosomes and regulates receptor recycling. *Mol. Biol. Cell* **20**, 5181–5194. doi:10.1091/mbc.e09-06-0535
- Solis, G. P., Hülsbusch, N., Radon, Y., Katanaev, V. L., Plattner, H. and Stuermer, C. A. O.** (2013). Reggies/flotillins interact with Rab11a and SNX4 at the tubulovesicular recycling compartment and function in transferrin receptor and E-cadherin trafficking. *Mol. Biol. Cell* **24**, 2689–2702. doi:10.1091/mbc.e12-12-0854
- Steinberg, F., Gallon, M., Winfield, M., Thomas, E. C., Bell, A. J., Heesom, K. J., Tavaré, J. M. and Cullen, P. J.** (2013). A global analysis of SNX27-retromer assembly and cargo specificity reveals a function in glucose and metal ion transport. *Nat. Cell Biol.* **15**, 461–471. doi:10.1038/ncb2721
- Sunio, A., Metcalf, A. B. and Krämer, H.** (1999). Genetic dissection of endocytic trafficking in *Drosophila* using a horseradish peroxidase-bridge of sevenless chimera: hook is required for normal maturation of multivesicular endosomes. *Mol. Biol. Cell* **10**, 847–859. doi:10.1091/mbc.10.4.847
- Szebenyi, G., Hall, B., Yu, R., Hashim, A. I. and Krämer, H.** (2007). Hook2 localizes to the centrosome, binds directly to centriolin/CEP110 and contributes to centrosomal function. *Traffic* **8**, 32–46. doi:10.1111/j.1600-0854.2006.00511.x
- Temkin, P., Lauffer, B., Jäger, S., Cimermancic, P., Krogan, N. J. and von Zastrow, M.** (2011). SNX27 mediates retromer tubule entry and endosome-to-plasma membrane trafficking of signalling receptors. *Nat. Cell Biol.* **13**, 715–721. doi:10.1038/ncb2252
- Walenta, J. H., Didier, A. J., Liu, X. and Krämer, H.** (2001). The Golgi-associated hook3 protein is a member of a novel family of microtubule-binding proteins. *J. Cell Biol.* **152**, 923–934. doi:10.1083/jcb.152.5.923
- Weigert, R., Yeung, A. C., Li, J. and Donaldson, J. G.** (2004). Rab22a regulates the recycling of membrane proteins internalized independently of clathrin. *Mol. Biol. Cell* **15**, 3758–3770. doi:10.1091/mbc.e04-04-0342
- Wu, B., Wang, Y., Yang, X.-M., Xu, B.-Q., Feng, F., Wang, B., Liang, Q., Li, Y., Zhou, Y., Jiang, J.-L. et al.** (2015). Basigin-mediated redistribution of CD98 promotes cell spreading and tumorigenicity in hepatocellular carcinoma. *J. Exp. Clin. Cancer Res.* **34**, 110. doi:10.1186/s13046-015-0226-6
- Wu, B., Zhou, Y., Wang, Y., Yang, X.-M., Liu, Z.-Y., Li, J.-H., Feng, F., Chen, Z.-N. and Jiang, J.-L.** (2016). Dominant Suppression of β 1 Integrin by Ectopic CD98-ICD Inhibits Hepatocellular Carcinoma Progression. *Int. J. Mol. Sci.* **17**, 1882. doi:10.3390/ijms17111882
- Xu, L., Sowa, M. E., Chen, J., Li, X., Gygi, S. P. and Harper, J. W.** (2008). An FTS/ Hook/p107(FHIP) complex interacts with and promotes endosomal clustering by the homotypic vacuolar protein sorting complex. *Mol. Biol. Cell* **19**, 5059–5071. doi:10.1091/mbc.e08-05-0473
- Yu, V. W., Ambartsoumian, G., Verlinden, L., Moir, J. M., Prud'homme, J., Gauthier, C., Roughley, P. J. and St-Arnaud, R.** (2005). FIAT represses ATF4-mediated transcription to regulate bone mass in transgenic mice. *J. Cell Biol.* **169**, 591–601. doi:10.1083/jcb.200412139
- Yu, V. W. C., Gauthier, C. and St-Arnaud, R.** (2008). FIAT represses bone matrix mineralization by interacting with ATF4 through its second leucine zipper. *J. Cell Biochem.* **105**, 859–865. doi:10.1002/jcb.21881
- Zhen, Y. and Stenmark, H.** (2015). Cellular functions of Rab GTPases at a glance. *J. Cell Sci.* **128**, 3171–3176. doi:10.1242/jcs.166074
- Zhou, S., Zhou, H., Walian, P. J. and Jap, B. K.** (2005). CD147 is a regulatory subunit of the gamma-secretase complex in Alzheimer's disease amyloid beta-peptide production. *Proc. Natl. Acad. Sci. USA* **102**, 7499–7504. doi:10.1073/pnas.0502768102

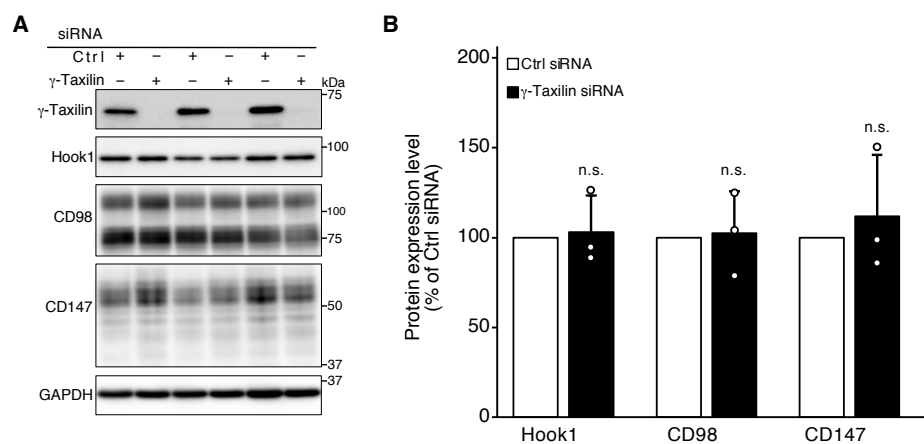


Fig. S1. γ -Taxilin depletion does not affect the expression levels of Hook1, CD98, or CD147 in HeLa cells.

(A) HeLa cells were transfected with control (Ctrl) or γ -taxilin (γ -Taxilin #1) siRNA. Cell lysates were subjected to SDS-PAGE followed by western blotting with the indicated antibodies.

(B) Quantitative analyses of protein expression levels in A. Results shown are the mean \pm SD of the ratio of each protein level in γ -taxilin-depleted cells to that in control cells ($n = 3$). n.s., not significant by two-tailed Student's *t*-test.

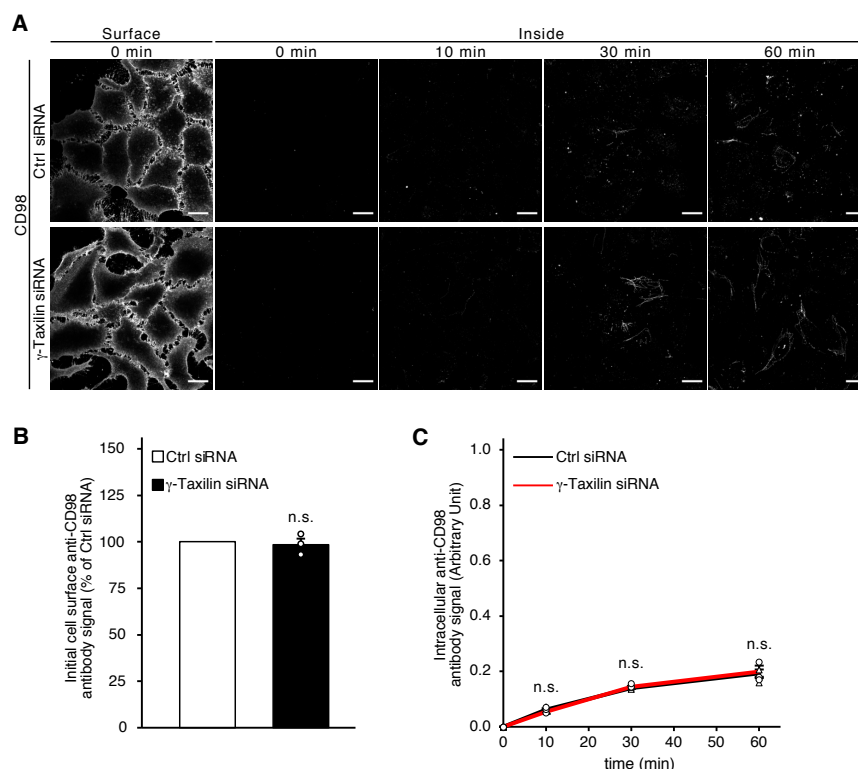


Fig. S2. γ -Taxilin depletion does not affect the internalization of CD98.

(A) Internalization of CD98. HeLa cells treated with the indicated siRNA were treated with anti-CD98 antibody for 1 h at 4°C. After washing out unbound antibody, the cells were incubated for the indicated time periods at 37°C. In the case of detection of surface anti-CD98 antibody at time zero, cells were fixed and stained without permeabilization. In the case of detection of internalized anti-CD98 antibody, surface anti-CD98 antibody was stripped by an acid wash. Then, the cells were fixed, permeabilized, and stained. Scale bars: 20 μ m.

(B,C) Quantitative analyses of anti-CD98 antibody signal in A. The intensity of anti-CD98 antibody signals was measured as signal intensity per μ m². In B, the results shown are the mean \pm s.e.m. of the ratio of the cell surface anti-CD98 antibody signal in γ -taxilin-depleted cells to that in control cells ($n = 3$; >40 cells were analyzed in each experiment). In C, the intensity of the cell surface anti-CD98 antibody signal at time zero was set to 1.0 for control and γ -taxilin-depleted cells, respectively. The results shown are the mean \pm s.e.m. of the ratio of the internalized anti-CD98 antibody signal at each time point to the cell surface anti-CD98 antibody signal at time zero ($n = 3$; >40 cells were analyzed in each experiment). n.s., not significant by two-tailed Student's *t*-test.

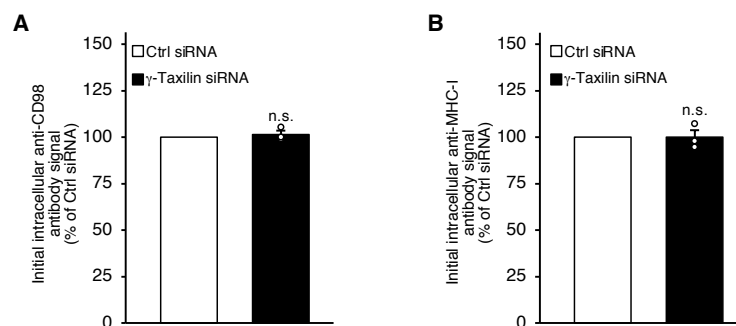


Fig. S3. γ -Taxilin depletion does not affect the amount of internalized CD98 and MHC-I at the starting point of the recycling assay in Fig 5.

(A,B) Quantitative analysis of internalized anti-CD98 and anti-MHC-I antibody signals. In A, the results shown are the mean \pm s.e.m. of the ratio of the anti-CD98 antibody signal in γ -taxilin-depleted cells at time zero to that in control cells at time zero ($n = 3$; >40 cells were analyzed in each experiment). In B, the results shown are the mean \pm s.e.m. of the ratio of the anti-MHC-I antibody signal in γ -taxilin-depleted cells at time zero to that in control cells at time zero ($n = 3$; >40 cells were analyzed in each experiment). n.s., not significant by two-tailed Student's t -test.

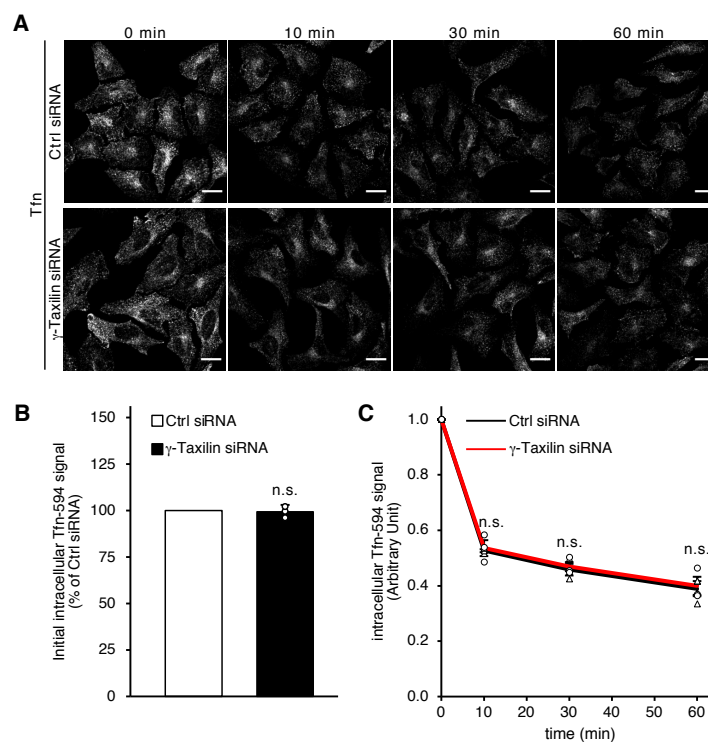


Fig. S4. γ -Taxilin depletion does not affect the recycling of TfnR.

(A) Recycling of TfnR. After serum starvation for 30 min at 37°C, HeLa cells treated with the indicated siRNA were incubated with Alexa Fluor 594-labeled Tfn (Tfn-594) for 1 h at 37°C. After washing out surface-bound Tfn-594, the cells were further incubated for the indicated time periods at 37°C and then fixed. Scale bars: 20 μ m.

(B,C) Quantitative analyses of Tfn-594 signal in A. The intensity of the Tfn-594 signal was measured as signal intensity per μ m². In B, the results shown are the mean \pm s.e.m. of the ratio of the Tfn-594 signal in γ -taxilin-depleted cells at time zero to that in control cells at time zero ($n = 3$; >40 cells were analyzed in each experiment). In C, the intensity of the Tfn-594 signal at time zero was set to 1.0 for control and γ -taxilin-depleted cells, respectively. The results shown are the mean \pm s.e.m. of the ratio of the Tfn-594 signal at each time point to that at time zero ($n = 3$; >40 cells were analyzed in each experiment). n.s., not significant by two-tailed Student's t -test.

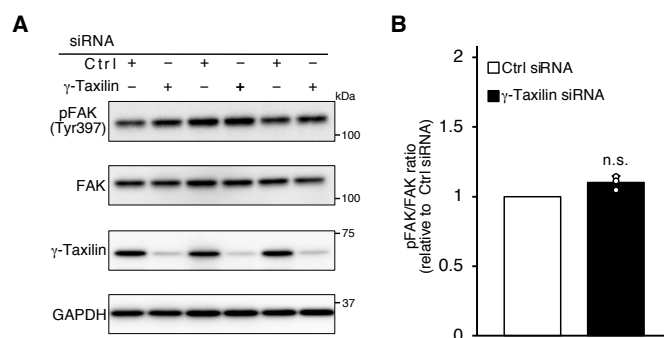


Fig. S5. γ -Taxilin depletion does not affect basal FAK phosphorylation levels in HeLa cells.

(A) HeLa cells were transfected with control (Ctrl) or γ -taxilin (γ -Taxilin #1) siRNA. Cell lysates were subjected to SDS-PAGE followed by western blotting with the indicated antibodies.

(B) Quantitative analysis of the phosphorylation of FAK on Tyr397 in A. The results shown are the mean \pm SD of the ratio of pFAK to FAK relative to that when using Ctrl siRNA ($n = 3$). n.s., not significant by two-tailed Student's t -test.

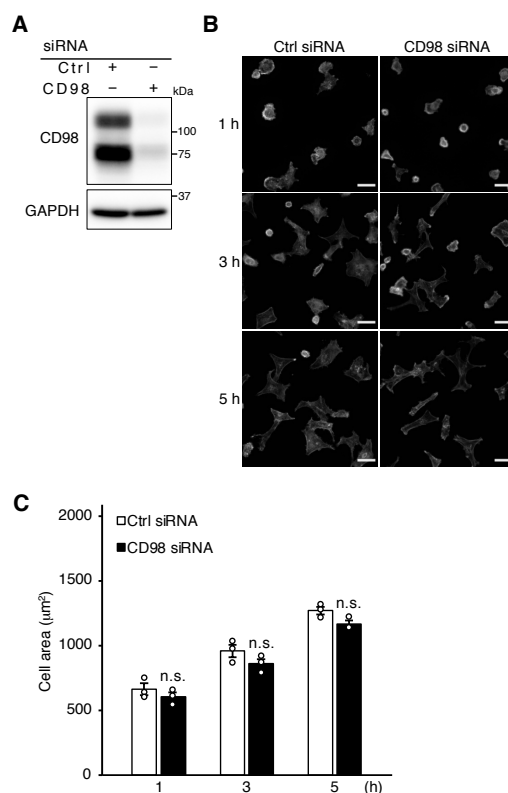


Fig. S6. CD98 depletion hardly affects cell spreading of HeLa cells.

(A) Depletion of CD98 by siRNA. HeLa cells were transfected with control (Ctrl) or CD98 siRNA. Cell lysates were subjected to SDS-PAGE followed by western blotting with the indicated antibodies.

(B) Cell spreading assay. HeLa cells treated with each siRNA were trypsinized and resuspended. The suspended cells were replated and incubated for the indicated time periods. Cells were visualized using Alexa Fluor 594-labeled phalloidin. Scale bars: 40 µm.

(C) Quantitative analysis of cell spreading in B. The area of spreading cells at each time point was measured. Data are expressed as the mean ± s.e.m. ($n = 3$; >100 cells were analyzed in each experiment). n.s., not significant by two-tailed Student's *t*-test.

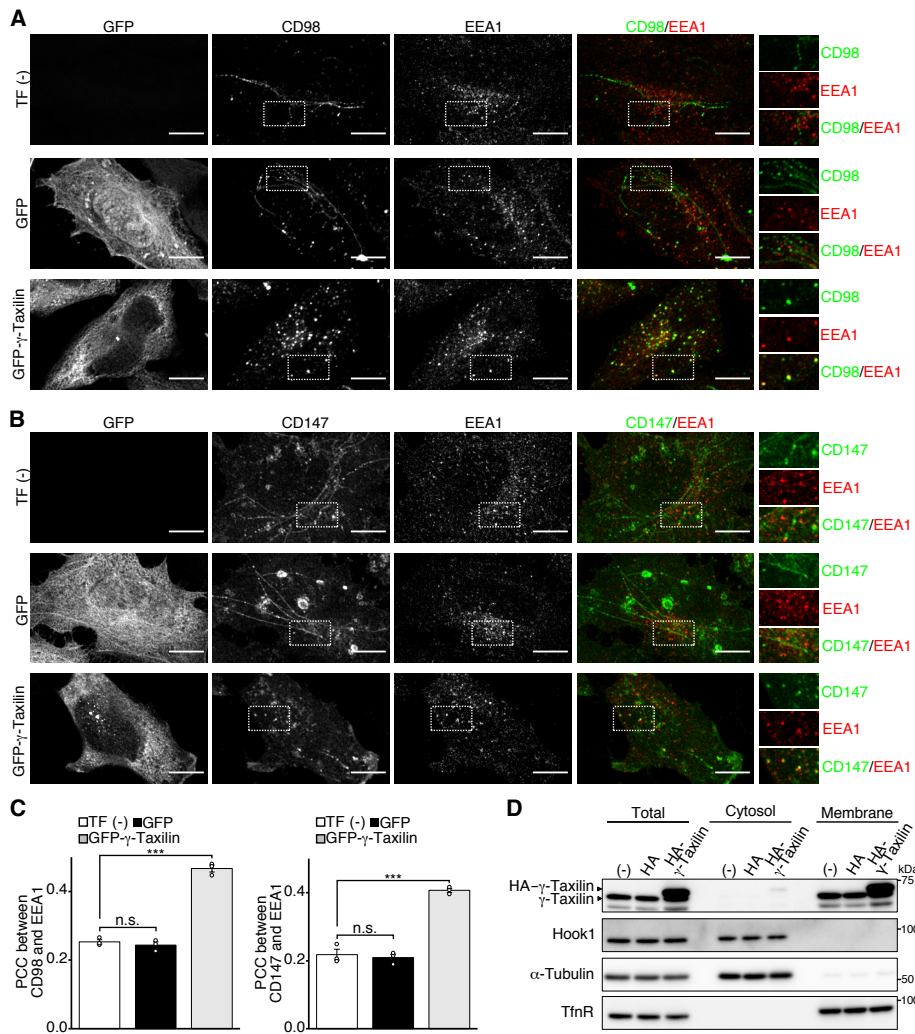


Fig. S7. Subcellular distribution of CD98, CD147, and Hook1 in cells overexpressing γ -taxilin.

(A,B) Subcellular distribution of CD98 and CD147. HeLa cells expressing GFP or GFP- γ -taxilin were subjected to the antibody uptake assay followed by immunostaining with an anti-EEA1 antibody. Scale bars: 10 μ m. Magnified views of the boxed areas in the panels are shown in the right panels.

(C) Pearson correlation coefficient (PCC) for the relation between CD98 or CD147 and EEA1 shown in A and B using the Fiji software. Data are expressed as the mean \pm s.e.m. ($n = 3$; >10 cells were analyzed in each experiment) ***, $P < 0.001$; n.s., not significant by one-way ANOVA with *post-hoc* Tukey's multiple comparison test.

(D) Subcellular fractionation of Hook1. The cytosolic and membrane fractions, and the total cell lysates of HeLa cells treated with the indicated plasmids were subjected to SDS-PAGE followed by western blotting with the indicated antibodies (n=3). TfnR and α -tubulin were used as markers for membrane and cytosolic proteins, respectively.

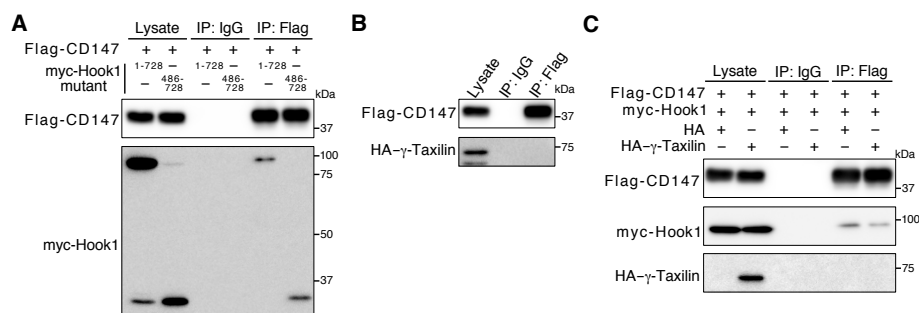
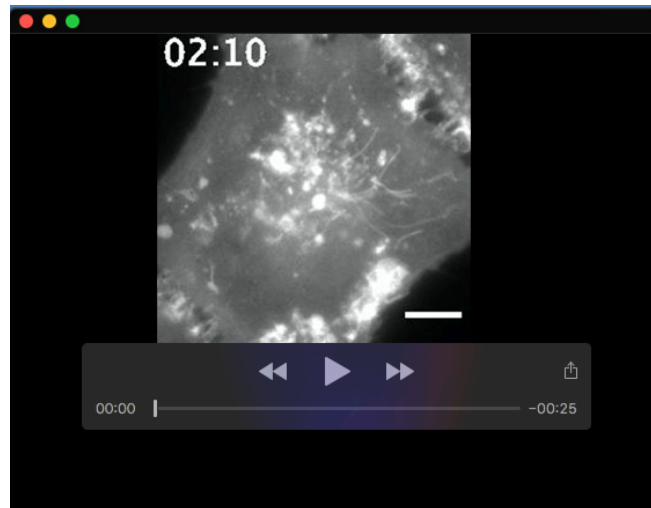


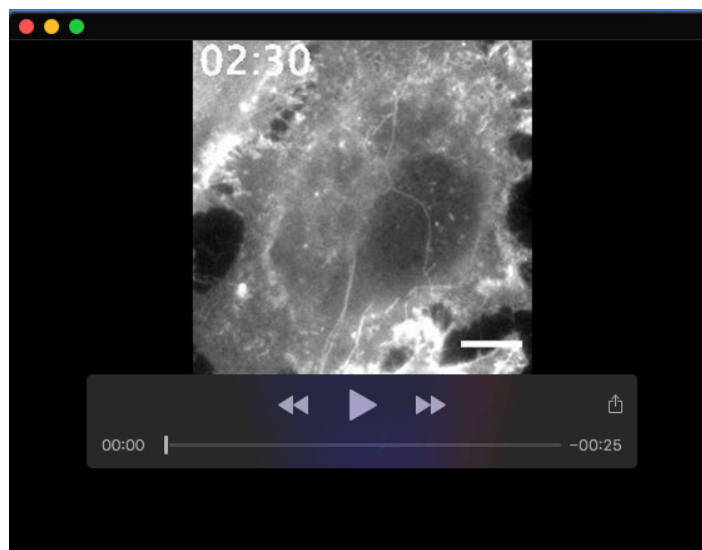
Fig. S8. γ -Taxilin binds to Hook1 competitively with CD147

(A-C) Co-immunoprecipitation assay. Cells were co-transfected with the indicated plasmids. Cell lysates were immunoprecipitated with the indicated antibodies. The immunoprecipitate was subjected to SDS-PAGE followed by western blotting with the indicated antibodies for detection of the corresponding proteins (n=3, each experiment). The amount of cell lysates used for western blotting were 2.5% of those used for IP.



Movie 1. Time-lapse imaging of Alexa Fluor 488-labelled anti-CD98 antibody in control siRNA-treated HeLa cells.

Time-lapse images were captured at 10-s intervals over 10 min. Scale bar: 10 μ m.



Movie 2. Time-lapse imaging of Alexa Fluor 488-labelled anti-CD98 antibody in γ -taxilin siRNA-treated HeLa cells.

Time-lapse images were captured at 10-s intervals over 10 min. Scale bar: 10 μ m.